

AS-ITP-98-09

hep-ph/9808379

Revised in Mar. 1999

Rare B Decays in Supersymmetry without R-parity

Tai-fu Feng *

Institute of Theoretical Physics, Academia Sinica, P. O. Box 2735, Beijing 100080, P.R.China

Abstract

We perform the complete computation of the contributions to $b \rightarrow s + \gamma$, $b \rightarrow se^+e^-$, $b \rightarrow s \sum \nu_i \bar{\nu}_i$ in supersymmetric model with bilinear R-parity violation. We compare our calculations with the evaluations in SM and the experimental results. We find that the supersymmetric contributions can be quite large in those processes. From the analysis and experimental results, we can get some constraints on the mass spectrum in the model.

PACS number(s): 12.60.Jv, 13.10.+q, 14.80.Ly

Typeset using REVTeX

*email: fengtf@itp.ac.cn

I. INTRODUCTION

It is being increasingly realized by those engaged in the search for the supersymmetry (SUSY) [1] that the principle of R-parity conservation, assumed to be sacrosanct in the prevalent search strategies, is not inviolable in practice. The R-parity of a particle is defined as $R = (-1)^{L+3B+2S}$, and can be violated if either baryon (B) or lepton (L) number is not conserved in nature, a fact perfectly compatible with the non observation of proton decay. Under R-parity violation the phenomenology changes considerably [2,3], the most important consequence is that the lightest supersymmetric particle (LSP) can decay now. However, the way in which R-parity can be violated is not unique. Different types of R-parity violating interaction terms can be written down, leading to different observable predictions. In addition, R-parity can be violated spontaneously, instead of explicitly, whence another class of interesting effects are expected [4]. If the phenomenology of R-parity breaking has to be understood, and the consequent modifications in the current search strategies have to be effectively implemented, then it is quite important to explore the full implication of each possible R-breaking scheme.

The R-conserving part of the minimal supersymmetric standard model (MSSM) is specified by the superpotential

$$\begin{aligned} \mathcal{W}_{MSSM} = & \mu \varepsilon_{ij} \hat{H}_i^1 \hat{H}_j^2 + \varepsilon_{ij} l_{IJ} \hat{H}_i^1 \hat{L}_j^I \hat{R}^J + \varepsilon_{ij} d_{IJ} \hat{H}_i^1 \hat{Q}_j^I \hat{D}^J \\ & + \varepsilon_{ij} u_{IJ} \hat{H}_i^2 \hat{Q}_j^I \hat{U}^J, \end{aligned} \quad (1)$$

where $I, J = 1, 2, 3$ are generation indices; $i, j = 1, 2$ are SU(2) indices; and ε is a completely antisymmetric 2×2 matrix, with $\varepsilon_{12} = 1$. The "hat" symbol over each letter indicates a superfield, \hat{Q}^I , \hat{L}^I , \hat{H}^1 , and \hat{H}^2 being SU(2) doublets with hyper-charges $\frac{1}{3}$, -1 , -1 , and 1 respectively; \hat{U} , \hat{D} and \hat{R} being SU(2) singlets with hyper-charges $-\frac{4}{3}$, $\frac{2}{3}$ and 2 respectively. The couplings u_{IJ} , d_{IJ} and l_{IJ} are 3×3 Yukawa matrices, and μ is parameter with unit of mass. If now the bilinear R-parity violating interactions are incorporated, the superpotential takes the form [5]

$$\mathcal{W} = \mathcal{W}_{MSSM} + \mathcal{W}_L \quad (2)$$

with $\mathcal{W}_L = \varepsilon_{ij}\epsilon'_I \hat{H}_i^2 \hat{L}_j^I$ and ϵ'_I is the parameter with unit of mass.

The soft SUSY-breaking terms:

$$\begin{aligned} \mathcal{L}_{soft} = & -m_{H^1}^2 H_i^{1*} H_i^1 - m_{H^2}^2 H_i^{2*} H_i^2 - m_{L^I}^2 \tilde{L}_i^{I*} \tilde{L}_i^I \\ & -m_{R^I}^2 \tilde{R}^{I*} \tilde{R}^I - m_{Q^I}^2 \tilde{Q}_i^{I*} \tilde{Q}_i^I - m_{D^I}^2 \tilde{D}^{I*} \tilde{D}^I \\ & -m_{U^I}^2 \tilde{U}^{I*} \tilde{U}^I + (m_1 \lambda_B \lambda_B + m_2 \lambda_A^i \lambda_A^i \\ & + m_3 \lambda_G^a \lambda_G^a + h.c.) + (B \mu \varepsilon_{ij} H_i^1 H_j^2 + B_I \epsilon'_I \varepsilon_{ij} H_i^2 \tilde{L}_j^I \\ & + \varepsilon_{ij} l_{sI} \mu H_i^1 \tilde{L}_j^I \tilde{R}^I + \varepsilon_{ij} d_{sI} \mu H_i^1 \tilde{Q}_j^I \tilde{D}^I \\ & + \varepsilon_{ij} u_{sI} \mu H_i^2 \tilde{Q}_j^I \tilde{U}^I + h.c.) \end{aligned} \quad (3)$$

where $m_{H^1}^2$, $m_{H^2}^2$, $m_{L^I}^2$, $m_{R^I}^2$, $m_{Q^I}^2$, $m_{D^I}^2$ and $m_{U^I}^2$ stand for the mass squared of the scalar fields while m_1 , m_2 , m_3 denote the masses of the $SU(3) \times SU(2) \times U(1)$ gauginos λ_G^a , λ_A^i and λ_B , B and B_I ($I = 1, 2, 3$) are free parameters with unit of mass.

\mathcal{W}_L and lepton-number breaking terms in \mathcal{L}_{soft} give a viable agent for R-parity breaking. It is particularly interesting for the fact that it can trigger a mixing between neutralinos and neutrinos as well as between charginos and charged leptons, resulting in observable effects. For ϵ'_3 can reach a large value (such as $|\epsilon'_3| \sim 500\text{GeV}$) even though we have considered the experimental fact that $m_\tau = 1.77\text{GeV}$ and $m_{\nu_\tau} \leq 24\text{MeV}$ [5], the mixing between charginos and charged leptons may give an important contribution to the rare B decays such as $b \rightarrow s + \gamma$, $b \rightarrow s e^+ e^-$, $b \rightarrow s \sum \nu_i \bar{\nu}_i$.

On the other hand, flavor-changing neutral current (FCNC) processes have constantly played a major role in the development of electroweak theories. FCNC studies have found kaon physics as their best research ground so far. However, the achievements in B-physics make B-mesons the new challenging frontier in the study of FCNC phenomena. At least some of the rare B-processes which are induced by the FCNC transitions $b \rightarrow s$ and $b \rightarrow d$ are within the reach of present machines. Needless to say, the test of such rare B-processes presents a probe of the validity of crucial ingredients of the Standard Model (SM) and,

possibly of the existence of new physics beyond the SM at the low energy scale.

$b \rightarrow s + \gamma$ and $b \rightarrow se^+e^-$ in the SM are analyzed in Ref [6,7]. The SM prediction for the branching ratio (Br) of the inclusive decay $b \rightarrow s + \gamma$, once the large QCD corrections are included [6], is a few times 10^{-4} . As for the semileptonic $b \rightarrow se^+e^-$ decay, the QCD-corrected SM prediction for its Br is about 10^{-6} [7].

FCNC rare B-processes have been widely analyzed as a potential probe for extensions of the SM implying new physics at the TeV scale. In the model with Two Higgs Doublets (THDM) and no tree level FCNC, the rare B decays and $B_d - \bar{B}_d$ mixing are computed in Ref [8, 9]. As for left-right symmetric models, the simplest choice of taking the CKM mixing angles in the right-handed sector equal to the corresponding left-handed ones (manifest or pseudo-manifest left-right symmetry) does not give any appreciable effects with respect to the SM estimates of rare B-processes [10]. Analogous results are obtained in the general case if no fine tunings of the parameters are allowed [11].

FCNC in the supersymmetry with R-parity has been discussed widely in Ref [12], Ref [13–15], FCNC in supersymmetry without R-parity has been discussed in Ref [16], the review of FCNC in the supersymmetric models can be found in Ref [17].

This paper is organized as follows. In sect. II, we give a description of the general structure of the supersymmetry with bilinear R-parity violation (BRPV). In sect. III, we provide the complete analyses to $b \rightarrow s + \gamma$, $b \rightarrow se^+e^-$, $b \rightarrow s \sum \nu_i \bar{\nu}_i$ in supersymmetric model with bilinear R-parity violation. In sect. IV, we perform a numerical analysis of those processes and compare them with the SM predictions and the experimental results. For completeness, we give the analytic expression for Feynman integrals which one encounters in the evaluation of the amplitudes listed in sect. III in appendix. A. A systematic notation for the relevant Feynman rules involving R-parity breaking terms are introduced in appendix. B. In appendix. C, we give the mass matrix of τ neutrino-neutralinos. For simplicity, we neglect the generation mixing of slepton and squark in the following analyses.

II. MINIMAL SUSY MODEL WITH BILINEAR R-PARITY VIOLATION

From the superpotential Eq. (2), we can perform an operation that is the same as in the standard model by redefinition of the fields [24]

$$\begin{aligned}
\hat{Q}_i^I &\rightarrow V_{Q_i}^{IJ} \hat{Q}_i^J, \\
\hat{U}^I &\rightarrow V_U^{IJ} \hat{U}^J, \\
\hat{D}^I &\rightarrow V_D^{IJ} \hat{D}^J, \\
\hat{L}_i^I &\rightarrow V_{L_i}^{IJ} \hat{L}_i^J, \\
\hat{R}^I &\rightarrow V_R^{IJ} \hat{R}^J.
\end{aligned} \tag{4}$$

One can diagonalize the matrices l_{IJ} , u_{IJ} and d_{IJ} , the superpotential has the form

$$\begin{aligned}
\mathcal{W} = & \mu \varepsilon_{ij} \hat{H}_i^1 \hat{H}_j^2 + l_I \varepsilon_{ij} \hat{H}_i^1 \hat{L}_j^I \hat{R}^I - u_I (\hat{H}_1^2 C^{JI*} \hat{Q}_2^J \\
& - \hat{H}_2^2 \hat{Q}_1^I) \hat{U}^I - d_I (\hat{H}_1^1 \hat{Q}_2^I - \hat{H}_2^1 C^{IJ} \hat{Q}_1^J) \hat{D}^I \\
& + \epsilon_I \varepsilon_{ij} \hat{H}_i^2 \hat{L}_j^I,
\end{aligned} \tag{5}$$

where C is the Kobayashi-Maskawa matrix and ϵ_I ($I = 1, 2, 3$) have the definition as:

$$\begin{aligned}
C &= V_{Q_2}^\dagger V_{Q_1}, \\
\epsilon_I &= \epsilon'_J V_L^{JI}.
\end{aligned} \tag{6}$$

The soft breaking sector has the form

$$\begin{aligned}
\mathcal{L}_{soft} = & -m_{H^1}^2 H_i^{1*} H_i^1 - m_{H^2}^2 H_i^{2*} H_i^2 - m_{L^I}^2 \tilde{L}_i^{I*} \tilde{L}_i^I - m_{R^I}^2 \tilde{R}^{I*} \tilde{R}^I \\
& - m_{Q^I}^2 \tilde{Q}_i^{I*} \tilde{Q}_i^I - m_{D^I}^2 \tilde{D}^{I*} \tilde{D}^I - m_{U^I}^2 \tilde{U}^{I*} \tilde{U}^I + (m_1 \lambda_B \lambda_B \\
& + m_2 \lambda_A^i \lambda_A^i + m_3 \lambda_G^a \lambda_G^a + h.c.) + \{ B \mu \varepsilon_{ij} H_i^1 H_j^2 + B_I \epsilon_I \varepsilon_{ij} H_i^2 \tilde{L}_j^I \\
& + \varepsilon_{ij} l_{sI} \mu H_i^1 \tilde{L}_j^I \tilde{R}^I + d_{sI} \mu (-H_1^1 \tilde{Q}_2^I + C^{IK} H_2^1 \tilde{Q}_1^K) \tilde{D}^I \\
& + u_{sI} \mu (-C^{KI*} H_1^2 \tilde{Q}_2^I + H_2^2 \tilde{Q}_1^I) \tilde{U}^I + h.c. \}.
\end{aligned} \tag{7}$$

For simplicity we take from now on $\epsilon_1 = \epsilon_2 = 0$, in this way, that only τ -lepton number is violated. The electroweak symmetry is broken when the two Higgs doublets H^1 , H^2 and the τ -slepton acquire vacuum expectation values (VEVs)

$$H^1 = \begin{pmatrix} \frac{1}{\sqrt{2}}(\chi_1^0 + v_1 + i\varphi_1^0) \\ H_2^1 \end{pmatrix} \quad (8)$$

$$H^2 = \begin{pmatrix} H_1^2 \\ \frac{1}{\sqrt{2}}(\chi_2^0 + v_2 + i\varphi_2^0) \end{pmatrix} \quad (9)$$

$$\tilde{L}_3 = \begin{pmatrix} \frac{1}{\sqrt{2}}(\chi_3^0 + v_3 + i\varphi_3^0) \\ \tilde{\tau}_L^- \end{pmatrix} \quad (10)$$

Note that the gauge bosons W and Z_0 acquire masses given by $m_W^2 = \frac{1}{4}g^2v^2$ and $m_Z^2 = \frac{1}{4}(g^2 + g'^2)v^2$, where $v^2 = v_1^2 + v_2^2 + v_3^2$ and g, g' are coupling constants of SU(2) and U(1). We introduce the following notation in spherical coordinates [3]

$$\begin{aligned} v_1 &= v \cos \theta_v \cos \beta, \\ v_2 &= v \sin \beta, \\ v_3 &= v \sin \theta_v \cos \beta. \end{aligned} \quad (11)$$

When the angle θ_v equals to zero, this sector will change back to the MSSM limit exactly. The massless neutral Goldstone boson can be written as:

$$G^0 = \cos \theta_v \cos \beta \varphi_1^0 - \sin \beta \varphi_2^0 + \sin \theta_v \cos \beta \varphi_3^0. \quad (12)$$

In the model with bilinear R-parity violation, the charged Higgs bosons mix with the left and right handed τ -slepton. In the original basis, where $\Phi_c = (H_2^{1*}, H_1^2, \tilde{\tau}_L^*, \tilde{\tau}_R)$, the scalar potential contains the following mass term

$$\mathcal{L}_m^C = -\Phi_c^\dagger \mathcal{M}_c^2 \Phi_c \quad (13)$$

with the symmetric matrix \mathcal{M}_c^2 is given by (here the matrix is too big to be written in full so we write it by each element individually)

$$\begin{aligned}
\mathcal{M}_{c1,1}^2 &= \frac{g^2}{4}(v_2^2 - v_3^2) + \frac{1}{2}v_3^2 l_3^2 + \epsilon_3 \mu \frac{v_3}{v_1} + B\mu \frac{v_2}{v_1}, \\
\mathcal{M}_{c1,2}^2 &= \frac{g^2}{4}v_1 v_2 + B\mu, \\
\mathcal{M}_{c1,3}^2 &= \frac{g^2}{4}v_1 v_3 - \epsilon_3 \mu - \frac{1}{2}l_3 v_1 v_3, \\
\mathcal{M}_{c1,4}^2 &= l_3 \epsilon_3 \frac{v_2}{\sqrt{2}} + l_{s3} \frac{\mu v_3}{\sqrt{2}}, \\
\mathcal{M}_{c2,2}^2 &= \frac{g^2}{4}(v_1^2 + v_3^2) - B_3 \epsilon_3 \frac{v_3}{v_2} + B\mu \frac{v_1}{v_2}, \\
\mathcal{M}_{c2,3}^2 &= \frac{g^2}{4}v_2 v_3 - B_3 \epsilon_3, \\
\mathcal{M}_{c2,4}^2 &= \frac{l_3}{\sqrt{2}} \mu v_3 + \frac{l_3}{\sqrt{2}} \epsilon_3 v_1, \\
\mathcal{M}_{c3,3}^2 &= \frac{g^2}{4}(v_2^2 - v_1^2) + \epsilon_3 \frac{\mu v_1}{v_3} - B_3 \frac{\epsilon_3 v_2}{v_3} + \frac{l_3^2}{2} v_1^2, \\
\mathcal{M}_{c3,4}^2 &= \frac{1}{\sqrt{2}} l_3 \mu v_2 - \frac{1}{\sqrt{2}} l_{s3} \mu v_1, \\
\mathcal{M}_{c4,4}^2 &= -\frac{g'^2}{4}(v_1^2 - v_2^2 + v_3^2) + \frac{1}{2} l_3^2 (v_1^2 + v_3^2) + m_{R^3}^2.
\end{aligned} \tag{14}$$

This matrix has an eigenstate:

$$\begin{aligned}
G^+ &= \sum_{i=1}^4 Z_H^{1,i} \Phi_c^i \\
&= \frac{1}{v} (v_1 H_2^{1*} - v_2 H_1^2 + v_3 \tilde{\tau}_L^*) \\
&= \cos \theta_v \cos \beta H_2^{1*} - \sin \beta H_1^2 + \sin \theta_v \cos \beta \tilde{\tau}_L^*
\end{aligned} \tag{15}$$

with zero eigenvalue, it is the massless charged Goldstone boson. In the physical (unitary) gauge, G^\pm are absorbed by W^\pm bosons and disappear from the Lagrangian. The other three eigenstates H^+ , $\tilde{\tau}_1$, $\tilde{\tau}_2$ can be expressed as:

$$\begin{aligned}
H^+ &= \sum_{i=1}^4 Z_H^{2,i} \Phi_c^i, \\
\tilde{\tau}_1 &= \sum_{i=1}^4 Z_H^{3,i} \Phi_c^i, \\
\tilde{\tau}_2 &= \sum_{i=1}^4 Z_H^{4,i} \Phi_c^i.
\end{aligned} \tag{16}$$

Similarly to the Higgs bosons, charginos mix with τ lepton forming a set of three charged

fermions $\tau, \tilde{\kappa}_2^-, \tilde{\kappa}_3^-$ [13,19]. In the original basis where $\psi^{+T} = (-i\lambda^+, \tilde{H}_2^1, \tau_R^+)$ and $\psi^{-T} = (-i\lambda^-, \tilde{H}_1^2, \tau_L^-)$, the charged fermion mass terms in the Lagrangian are

$$\mathcal{L}_m = -\psi^{-T} \mathcal{M}_f \psi^+ + h.c. \quad (17)$$

with the mass matrix is given by [13,19]:

$$\mathcal{M}_f = \begin{pmatrix} 2m_2 & \frac{ev_2}{\sqrt{2}s_W} & 0 \\ \frac{ev_1}{\sqrt{2}s_W} & \mu & \frac{l_3 v_3}{\sqrt{2}} \\ \frac{ev_3}{\sqrt{2}s_W} & \epsilon_3 & \frac{l_3 v_1}{\sqrt{2}} \end{pmatrix} \quad (18)$$

where $S_W = \sin \theta_W$ and $\lambda^\pm = \frac{\lambda_A^1 \mp i\lambda_A^2}{\sqrt{2}}$. Also the two mixing matrices Z^+ and Z^- appear in the Lagrangian, they are defined by the condition that the product $(Z^+)^T \mathcal{M}_f Z^-$ should be diagonal

$$(Z^+)^T \mathcal{M}_f Z^- = \begin{pmatrix} m_{\tilde{\kappa}_1^-} & 0 & 0 \\ 0 & m_{\tilde{\kappa}_2^-} & 0 \\ 0 & 0 & m_{\tilde{\kappa}_3^-} \end{pmatrix} \quad (19)$$

Here, we assume $m_{\tilde{\kappa}_1^-} = m_\tau$ and $m_{\tilde{\kappa}_3^-} > m_{\tilde{\kappa}_2^-} > m_{\tilde{\kappa}_1^-}$.

III. COMPLETE ANALYSIS OF THE RARE B-PROCESSES IN SUSY MODEL WITH BILINEAR R-PARITY VIOLATION

Because we neglect the generation mixing of sleptons and squarks, there are no the couplings such as $\bar{\kappa}_i^0 \gamma_\mu P_{L,R} q_u^I \tilde{U}_{1,2}^J$ ($I \neq J$), $\bar{\kappa}_i^0 \gamma_\mu P_{L,R} q_d^I \tilde{D}_{1,2}^J$ ($I \neq J$), $\bar{\kappa}_i^0 \gamma_\mu P_{L,R} e^I \tilde{E}_{1,2}^J$ ($I \neq J$), $\bar{\lambda}_G^a \gamma_\mu P_{L,R} q_u^I \tilde{U}_{1,2}^J$ ($I \neq J$) and $\bar{\lambda}_G^a \gamma_\mu P_{L,R} q_d^I \tilde{D}_{1,2}^J$ ($I \neq J$) where $I, J = 1, 2, 3$ are the generational indices and $\kappa_1^0, \kappa_2^0, \kappa_3^0, \kappa_4^0, \lambda_G^a$ represent the neutralinos and gluinos. Under this assumption, the contribution of gluino and neutralino is zero when we compute the rare processes such as $b \rightarrow s + \gamma$, $b \rightarrow s + e^+ e^-$ and $b \rightarrow s + \sum \nu_i \bar{\nu}_i$ at one loop level.

In this section, we will use the effective Hamiltonian theory to discuss those processes. The method of the effective Hamiltonian theory was first used by Ref [18] and has been

developed over the last years [25] [26]. It is a two step program, starting with an operator product expansion (OPE) and performing a renormalization group equation (RGE) analysis afterwards. The derivation starts as follows: if the kinematics of the decay are of the kind that the masses of the internal particles m_i are much larger than the external momentum p : $m_i^2 \gg p^2$, then the heavy particles can be integrated out. This concept takes a concrete form with the functional integral formalism. It means that the heavy particles are removed as dynamical degrees of freedom from the theory, hence their fields do not appear in the (effective) Lagrangian anymore. Their residual effect lies in the generated effective vertices. In this way an effective low energy theory can be constructed from the full theory. In the framework of the standard model, strong interactions are known to give sizable contributions to FCNC processes, the inclusion of the QCD corrections increases the electroweak rate by about a factor two for $b \rightarrow s\gamma$ process, and enhances the rate about 30% for $b \rightarrow se^+e^-$ transition [27]. Now, let us derive the effective Lagrangian for $b \rightarrow s\gamma$, $b \rightarrow se^-e^+$ and $b \rightarrow s \sum \nu_i \bar{\nu}_i$ first (at the M_W scale), then we analyze the renormalization group equation (RGE) in the leading logarithmic approximation (LLA), i.e. to sum up the terms $[\alpha_s \ln(\frac{M_W}{\mu})]^n$ to all orders n ($n=0, 1, \dots, \infty$) in perturbation theory.

A. The $b\bar{s}Z$, $b\bar{s}\gamma$ couplings and box diagrams in SUSY model with bilinear R-parity violation

We follow the method that was used in Ref [18]. In the 't Hooft Feynman gauge, the one-loop diagrams for the induced $b\bar{s}Z$ coupling are shown in Fig. 1. The diagrams Fig. 1(a), Fig. 1(b) and Fig. 1(c) represent the SM contribution of the $b \rightarrow s$ transition. In each group, the first two diagrams (except for Fig. 1(c)) are self-energy part. Since the weak current is not conserved, we only need to expect a non-vanishing zeroth-order contribution in the momentum q (q denotes the momentum transfer through the Z-boson). The induced $b\bar{s}Z$ coupling takes the form:

$$\Gamma_{Z_\mu}^{(i)} = \bar{s}\gamma_\mu P_L b \Gamma^{(i)} \quad (20)$$

where $i = a, b, c, d, e$ and $P_{L,R} = \frac{1 \mp \gamma_5}{2}$. The Γ^i can be written as (at the M_W scale):

$$\Gamma^{(a)} = \frac{e^3}{(4\pi)^2 \sin^3 \theta_W \cos \theta_W} C_{ts}^* C_{tb} \left\{ \left(\frac{1}{2} - \frac{1}{3} \sin^2 \theta_W \right) [2f_2^{(0)}(x_{tw}) - 4f_{3b}^{(1)}(x_{tw})] - \left(\frac{1}{4} - \frac{1}{3} \sin^2 \theta_W \right) f_{3b}^{(1)}(x_{tw}) - \frac{2}{3} \sin^2 \theta_W x_{tw} f_{3b}^{(0)}(x_{tw}) + \frac{3}{2} \cos^2 \theta_W f_{3a}^{(1)}(x_{tw}) \right\}, \quad (21)$$

$$\Gamma^{(b)} = \frac{e^3}{(4\pi)^2 \sin^3 \theta_W \cos \theta_W} C_{ts}^* C_{tb} \left\{ \left(\frac{1}{2} - \frac{1}{3} \sin^2 \theta_W \right) \frac{x_{tw}}{2} [f_2^{(0)}(x_{tw}) - 2f_{3b}^{(1)}(x_{tw})] + \frac{x_{tw}}{2} \left[\left(\frac{1}{2} - \frac{2}{3} \sin^2 \theta_W \right) x_{tw} f_{3b}^{(0)}(x_{tw}) + \frac{1}{3} \sin^2 \theta_W f_{3b}^{(1)}(x_{tw}) \right] + \frac{x_{tw}}{8} (\cos^2 \theta_W - \sin^2 \theta_W) f_{3a}^{(1)}(x_{tw}) \right\}, \quad (22)$$

$$\Gamma^{(c)} = \frac{e^3}{(4\pi)^2 \sin^3 \theta_W \cos \theta_W} C_{ts}^* C_{tb} \sqrt{2} \sin^2 \theta_W x_{tw} f_{3a}^{(0)}(x_{tw}), \quad (23)$$

$$\Gamma^{(d)} = \frac{e^3}{(4\pi)^2 \sin^3 \theta_W \cos \theta_W} C_{ts}^* C_{tb} \left\{ \left(\frac{1}{2} - \frac{1}{3} \sin^2 \theta_W \right) \frac{x_{tw}}{2 \sin^2 \theta_v \sin^2 \beta} \sum_{i=2}^4 Z_H^{2i} Z_H^{2i*} [f_2^{(0)}(x_{ts_i}) - 2f_{3b}^{(1)}(x_{ts_i})] + \frac{x_{tw}}{2 \sin^2 \theta_v \sin^2 \beta} \sum_{i=2}^4 Z_H^{2i} Z_H^{2i*} \left[\left(\frac{1}{2} - \frac{2}{3} \sin^2 \theta_W \right) x_{ts_i} f_{3b}^{(0)}(x_{ts_i}) + \frac{1}{3} \sin^2 \theta_W f_{3b}^{(1)}(x_{ts_i}) \right] - \frac{x_{tw}}{8 \sin \theta_v \sin \beta} \sum_{i=2}^4 \sum_{j=2}^4 Z_H^{2i} Z_H^{2j*} [(\cos^2 \theta_W - \sin^2 \theta_W) \delta_{ij} - Z_H^{4i} Z_H^{4j*}] f_{3c}^{(1)}(x_{ts_i}, x_{s_j s_i}) \right\}, \quad (24)$$

$$\Gamma^{(e)} = \frac{e^3}{(4\pi)^2 \sin^3 \theta_W \cos \theta_W} C_{ts}^* C_{tb} \left\{ \sum_{i=1}^2 \sum_{j=1}^3 \left| (-Z_{\tilde{Q}^3}^{1i*} Z_{1j}^+ + \frac{Z_{\tilde{Q}^3}^{2i*} Z_{2j}^+}{\sqrt{2} M_W \sin \theta_v \sin \beta}) \right|^2 \left(\frac{1}{2} - \frac{1}{3} \sin^2 \theta_W \right) [f_2^{(0)}(x_{\tilde{\kappa}_j^- \tilde{t}_i}) - 2f_{3b}^{(1)}(x_{\tilde{\kappa}_j^- \tilde{t}_i})] + \sum_{i,l=1}^2 \sum_{j=1}^3 \left(-Z_{\tilde{Q}^3}^{1i*} Z_{1j}^+ + \frac{m_t Z_{\tilde{Q}^3}^{2i*} Z_{2j}^+}{\sqrt{2} M_W \sin \theta_v \sin \beta} \right) \left(-Z_{\tilde{Q}^3}^{1l} Z_{1j}^{+*} + \frac{m_t Z_{\tilde{Q}^3}^{2l} Z_{2j}^{+*}}{\sqrt{2} M_W \sin \theta_v \sin \beta} \right) \left(-\frac{1}{4} Z_{\tilde{Q}^3}^{1i*} Z_{\tilde{Q}^3}^{1i} - \frac{1}{3} \sin^2 \theta_W \delta_{il} \right) f_{3c}^{(0)}(x_{\tilde{\kappa}_j^- \tilde{t}_i}, x_{\tilde{t}_l \tilde{t}_i}) + \sum_{i,j=1}^3 \sum_{l=1}^2 \frac{1}{2} \left(-Z_{\tilde{Q}^3}^{1l} Z_{1j}^{+*} + \frac{m_t Z_{\tilde{Q}^3}^{2l} Z_{2j}^{+*}}{\sqrt{2} M_W \sin \theta_v \sin \beta} \right) \left(-Z_{\tilde{Q}^3}^{1i*} Z_{1j}^+ + \frac{m_t Z_{\tilde{Q}^3}^{2i*} Z_{2j}^+}{\sqrt{2} M_W \sin \theta_v \sin \beta} \right) [(Z_{1j}^- Z_{1i}^{+*} + 2\delta_{ij} \cos 2\theta_W) \frac{1}{2} f_{3c}^{(1)}(x_{\tilde{\kappa}_i^- \tilde{t}_l}, x_{\tilde{\kappa}_j^- \tilde{t}_l}) + x_{\tilde{\kappa}_i^- \tilde{t}_l} x_{\tilde{\kappa}_j^- \tilde{t}_l} (Z_{1j}^{+*} Z_{1i}^+ + 2\delta_{ij} \cos 2\theta_W) f_{3c}^{(0)}(x_{\tilde{\kappa}_i^- \tilde{t}_l}, x_{\tilde{\kappa}_j^- \tilde{t}_l})] \right\}, \quad (25)$$

where $s_{i=1,2,3,4} = (G^-, H^-, \tilde{t}_1, \tilde{t}_2)$ and $x_{\alpha\beta} = \frac{m_\alpha^2}{m_\beta^2}$. $Z_{\tilde{Q}^3}$ is the top-squark mixing matrix, its definition can be found in appendix. B.

Notice that the ultraviolet divergences cancel separately for each of those equation. In

obtaining the form shown, the unitary property of Z_H , $Z_{\tilde{Q}^3}$, Z^+ and Z^- has been used, together with the unitarity of the Kobayashi-Maskawa matrix.

The computation of the photon exchanged contribution is somewhat more involved and requires the calculation of the induced $b\bar{s}\gamma$ coupling up to second order in the external momentum. The diagrams need to be computed are those of Fig. 1 with Z being replaced by γ . The induced $b\bar{s}\gamma$ coupling takes the form (at the M_W scale):

$$\Gamma_{\gamma\mu}^{(i)} = \bar{s}[F_1^{(i)}(q^2\gamma_\mu - q_\mu\not{q})P_L + F_2^{(i)}\not{q}\gamma_\mu(m_sP_L + m_bP_R)]b \quad (26)$$

where $i = a, b, c, d, e$ and

$$F_1^{(a)} = \frac{1}{(4\pi)^2} \frac{e^3}{\sin^2 \theta_W} C_{tb} C_{ts}^* \frac{1}{M_W^2} \left\{ \frac{1}{9} f_{5d}^{(2)}(x_{tw}) - \frac{2}{3} f_{4c}^{(1)}(x_{tw}) + \right. \\ \left. \frac{1}{2} f_{3a}^{(0)}(x_{tw}) + \frac{1}{2} f_{4b}^{(1)}(x_{tw}) - \frac{3}{2} f_{4a}^{(1)}(x_{tw}) + \right. \\ \left. \frac{4}{3} f_{5a}^{(2)}(x_{tw}) - \frac{1}{3} f_{5b}^{(2)}(x_{tw}) \right\}, \quad (27)$$

$$F_2^{(a)} = \frac{1}{(4\pi)^2} \frac{e^3}{\sin^2 \theta_W} C_{tb} C_{ts}^* \frac{1}{M_W^2} \left\{ \frac{2}{3} f_{3b}^{(0)}(x_{tw}) - f_{4c}^{(1)}(x_{tw}) + \right. \\ \left. \frac{1}{3} f_{5d}^{(2)}(x_{tw}) + \frac{1}{2} f_{3a}^{(0)}(x_{tw}) - \frac{3}{2} f_{4b}^{(1)}(x_{tw}) - \right. \\ \left. \frac{1}{4} f_{4a}^{(1)}(x_{tw}) + \frac{1}{3} f_{5c}^{(2)}(x_{tw}) + \frac{1}{3} f_{5b}^{(2)}(x_{tw}) + \frac{2}{9} \left[\frac{\ln x_{tw}}{x_{tw} - 1} \right. \right. \\ \left. \left. + \ln \frac{m_c^2}{M_W^2} + f\left(\frac{q^2}{m_b^2}\right) \right] \right\}, \quad (28)$$

$$F_1^{(b)} = \frac{1}{(4\pi)^2} \frac{e^3}{\sin^2 \theta_W} C_{tb} C_{ts}^* \frac{1}{M_W^2} \left\{ -\frac{x_{tw}}{18} f_{5d}^{(2)}(x_{tw}) - \frac{x_{tw}}{12} f_{5c}^{(2)}(x_{tw}) + \right. \\ \left. \frac{x_{tw}}{12} f_{5b}^{(2)}(x_{tw}) \right\}, \quad (29)$$

$$F_2^{(b)} = \frac{1}{(4\pi)^2} \frac{e^3}{\sin^2 \theta_W} C_{tb} C_{ts}^* \frac{1}{M_W^2} \left\{ \frac{x_{tw}}{2} f_{4c}^{(1)}(x_{tw}) - \frac{x_{tw}}{6} f_{5d}^{(2)}(x_{tw}) + \right. \\ \left. \frac{3x_{tw}}{8} f_{4b}^{(1)}(x_{tw}) - \frac{1}{6} f_{5c}^{(2)}(x_{tw}) - \right. \\ \left. \frac{1}{12} f_{5b}^{(2)}(x_{tw}) \right\}, \quad (30)$$

$$F_1^{(c)} = -\frac{1}{(4\pi)^2} \frac{e^3}{\sin^2 \theta_W} C_{tb} C_{ts}^* \frac{x_{tw}}{M_W^2} f_{5a}^{(2)}(x_{tw}), \quad (31)$$

$$F_2^{(c)} = \frac{1}{(4\pi)^2} \frac{e^3}{\sin^2 \theta_W} C_{tb} C_{ts}^* \frac{1}{4M_W^2} f_{4a}^{(1)}(x_{tw}), \quad (32)$$

$$F_1^{(d)} = \frac{1}{(4\pi)^2} \frac{e^3}{\sin^2 \theta_W} C_{tb} C_{ts}^* \sum_{i=2}^4 \frac{Z_H^{2i} Z_H^{2i*}}{6M_W^2 \sin^2 \theta_W \sin^2 \beta} \left\{ -\frac{1}{3} f_{5d}^{(2)}(x_{ts_i}) - \right.$$

$$\frac{1}{2}f_{5c}^{(2)}(x_{ts_i}) + \frac{1}{2}f_{5b}^{(2)}(x_{ts_i})\}, \quad (33)$$

$$\begin{aligned} F_2^{(d)} = & \frac{1}{(4\pi)^2} \frac{e^3}{\sin^2 \theta_W} C_{tb} C_{ts}^* \sum_{i=2}^4 \left\{ \frac{x_{ts_i}}{6M_W^2 \sin^2 \theta_W} \left[\left(\frac{Z_H^{2i} Z_H^{2i*}}{\sin^2 \beta} + 2 \frac{Z_H^{1i*} Z_H^{2i}}{\sin \beta \cos \beta} \right) f_{4c}^{(1)}(x_{ts_i}) - \right. \right. \\ & \frac{Z_H^{2i} Z_H^{2i*}}{\sin^2 \beta} f_{5d}^{(2)}(x_{ts_i}) \left. \right] + \frac{x_{ts_i}}{2M_W^2 \sin^2 \theta_v} \left[\frac{Z_H^{2i} Z_H^{2i*}}{4 \sin^2 \beta} f_{4b}^{(1)}(x_{ts_i}) + \right. \\ & \frac{Z_H^{1i*} Z_H^{2i}}{2 \sin \beta \cos \beta} f_{4b}^{(1)}(x_{ts_i}) - \frac{Z_H^{2i} Z_H^{2i*}}{3 \sin^2 \beta} f_{5c}^{(2)}(x_{ts_i}) - \\ & \left. \left. \frac{Z_H^{2i} Z_H^{2i*}}{6 \sin^2 \beta} f_{5b}^{(2)}(x_{ts_i}) \right] \right\}, \quad (34) \end{aligned}$$

$$\begin{aligned} F_1^{(e)} = & \frac{1}{(4\pi)^2} \frac{e^3}{\sin^2 \theta_W} C_{tb} C_{ts}^* \sum_{i=1,2} \sum_{j=1}^3 \frac{1}{m_{\tilde{t}_i}^2} \left| Z_{\tilde{Q}^3}^{1i} Z_{1,j}^{+*} - \frac{m_t Z_{\tilde{Q}^3}^{2i} Z_{2j}^{+*}}{\sqrt{2} M_W \sin \theta_v \sin \beta} \right|^2 \left\{ \frac{2}{9} f_{5a}^{(2)}(x_{\tilde{\kappa}_j^- \tilde{t}_i}) + \right. \\ & \left. \frac{1}{6} f_{5d}^{(2)}(x_{\tilde{\kappa}_j^- \tilde{t}_i}) \right\}, \quad (35) \end{aligned}$$

$$\begin{aligned} F_2^{(e)} = & \frac{1}{(4\pi)^2} \frac{e^3}{\sin^2 \theta_W} C_{tb} C_{ts}^* \sum_{i=1,2} \sum_{j=1}^3 \frac{1}{m_{\tilde{t}_i}^2} \left\{ \left| Z_{\tilde{Q}^3}^{1i} Z_{1,j}^{+*} - \frac{m_t Z_{\tilde{Q}^3}^{2i} Z_{2j}^{+*}}{\sqrt{2} M_W \sin \theta_v \sin \beta} \right|^2 \left[-\frac{1}{2} f_{4c}^{(1)}(x_{\tilde{\kappa}_j^- \tilde{t}_i}) + \right. \right. \\ & \frac{1}{2} f_{5d}^{(2)}(x_{\tilde{\kappa}_j^- \tilde{t}_i}) - \frac{2}{3} f_{4b}^{(1)}(x_{\tilde{\kappa}_j^- \tilde{t}_i}) + \frac{2}{9} f_{5c}^{(2)}(x_{\tilde{\kappa}_j^- \tilde{t}_i}) - \\ & \frac{1}{18} f_{5b}^{(2)}(x_{\tilde{\kappa}_j^- \tilde{t}_i}) \left. \right] - \frac{1}{2} (Z_{\tilde{Q}^3}^{1i} Z_{1,j}^{+*} + \frac{m_t Z_{\tilde{Q}^3}^{2i} Z_{2j}^{+*}}{\sqrt{2} M_W \sin \theta_v \sin \beta}) \frac{Z_{\tilde{Q}^3}^{1i*} Z_{2j}^{-*} m_{\tilde{\kappa}_j}}{\sqrt{2} M_W \sin \theta_v \cos \beta} \\ & \left. \left[f_{4c}^{(1)}(x_{\tilde{\kappa}_j^- \tilde{t}_i}) + \frac{2}{3} f_{4b}^{(1)}(x_{\tilde{\kappa}_j^- \tilde{t}_i}) \right] \right\}. \quad (36) \end{aligned}$$

The function $f(s)$ is defined as

$$f(s) = -\frac{2}{3} - \frac{z}{s} + \begin{cases} 2(1 + \frac{z}{2s}) \sqrt{\frac{z}{s} - 1} \tan^{-1} [\sqrt{\frac{z}{s} - 1}]^{-1}, & \text{if } s < z, \\ (1 + \frac{z}{2s}) \sqrt{1 - \frac{z}{s}} [\ln \frac{1 + \sqrt{1 - z/s}}{1 - \sqrt{1 - z/s}} - i\pi], & \text{if } s > z \end{cases} \quad (37)$$

where $z = \frac{4m_c^2}{m_b^2}$ and $f(0) = 1$. The other functions are given in appendix. A.

The box-diagrams that contribute to the $b \rightarrow se^+e^-$ are shown in Fig. 2. The effective Lagrangian takes the form (at the M_W scale):

$$A_i^{box} (\bar{s} \gamma^\mu P_L b) (\bar{e} \gamma_\mu P_L e) \quad (38)$$

with

$$\begin{aligned} A_a^{box} = & \frac{1}{(4\pi)^2} \frac{e^4}{4 \sin^4 \theta_W} C_{ts}^* C_{tb} \frac{1}{M_W^2} f_{4d}^{(1)}(x_{tw}, 0), \\ A_b^{box} = & \frac{1}{(4\pi)^2} \frac{e^4}{4 \sin^4 \theta_W} C_{ts}^* C_{tb} \sum_{i,j=1}^3 \sum_{l=1}^2 \frac{1}{m_{\tilde{t}_i}^2} Z_{1j}^{+*} Z_{1i}^+ (-Z_{\tilde{Q}^3}^{1l*} Z_{1j}^+ + \frac{m_t Z_{\tilde{Q}^3}^{2l*} Z_{2i}^+}{\sqrt{2} M_W \sin \theta_v \sin \beta}) \end{aligned} \quad (39)$$

$$(-Z_{\tilde{Q}^3}^{1l}Z_{1j}^{+*} + \frac{m_t Z_{\tilde{Q}^3}^{2l} Z_{2i}^{+*}}{\sqrt{2}M_W \sin \theta_v \sin \beta})f_{4e}^{(1)}(x_{\tilde{\kappa}_j^- \tilde{t}_l}, x_{\tilde{\kappa}_i^- \tilde{t}_l}, x_{\tilde{\nu}_e \tilde{t}_l}). \quad (40)$$

As for $b \rightarrow s\nu_e \bar{\nu}_e$, it is analogous with the case of $b \rightarrow se^+e^-$. The box diagrams that contribute to the $b \rightarrow s\nu_e \bar{\nu}_e$ are given in Fig. 3. The effective Lagrangian takes the form (at the M_W scale):

$$B_i^{box}(\bar{s}\gamma^\mu P_L b)(\bar{\nu}_e \gamma_\mu P_L \nu_e) \quad (41)$$

with

$$\begin{aligned} B_a^{box} &= \frac{1}{(4\pi)^2} \frac{e^4}{4 \sin^4 \theta_W} C_{ts}^* C_{tb} \frac{1}{M_W^2} f_{4d}^{(1)}(x_{eW}, x_{tw}), \\ B_b^{box} &= \frac{1}{(4\pi)^2} \frac{e^4}{4 \sin^4 \theta_W} C_{ts}^* C_{tb} \frac{1}{m_{\tilde{t}_l}^2} \sum_{h=1,2} \sum_{i,j} \sum_{l=1,2} Z_{\tilde{E}^1}^{1h} Z_{\tilde{E}^1}^{1h*} Z_{1i}^- Z_{1j}^{-*} \\ &\quad | - Z_{\tilde{Q}^3}^{1l*} Z_{1i}^+ + \frac{m_t Z_{\tilde{Q}^3}^{2l*} Z_{2i}^+}{\sqrt{2}M_W \sin \theta_v \sin \beta} |^2 f_{4e}^{(1)}(x_{\tilde{\kappa}_i^- \tilde{t}_l}, x_{\tilde{\kappa}_j^- \tilde{t}_l}, x_{\tilde{e}_h^- \tilde{t}_l}) \end{aligned} \quad (42)$$

$$(43)$$

where $Z_{\tilde{E}^I}$ is the mixing matrix of slepton ($I=1, 2$ is the index of generation), its definition can be found in appendix. B.

B. The width of $b \rightarrow s + \gamma$ in SUSY model with bilinear R-parity violation

The total amplitude of the decay $b \rightarrow s + \gamma$ can therefore be written as:

$$\mathcal{A}_{tot}^\gamma(b \rightarrow s + \gamma) = F_2 \mathcal{O}_{LR}^\gamma \quad (44)$$

with F_2 is the sum of Eq. (28), Eq. (30), Eq. (32), Eq. (34), Eq. (36). Where $\mathcal{O}_{LR}^\gamma = m_b \epsilon_\mu \bar{s} \not{d} \gamma^\mu P_R b$ and the contribution of $\mathcal{O}_{RL}^\gamma = m_s \epsilon_\mu \bar{s} \not{d} \gamma^\mu P_L b$ is neglected since it is order of $O(\frac{m_s^2}{m_b^2})$.

By denoting the total amplitude at a scale μ as $F_2(\mu)$, the QCD- corrected amplitude at the scale of the process ($\sim m_b$) is then given by [15]

$$F_2(m_b) = \eta^{-\frac{16}{23}} \{ F_2(M_W) + F_2^0 [\frac{116}{135} (\eta^{\frac{10}{23}} - 1) + \frac{58}{189} (\eta^{\frac{28}{23}} - 1)] \}, \quad (45)$$

where

$$\eta = \alpha_s(m_b)/\alpha_s(M_W) \approx 1.8,$$

$$F_2^0 = \frac{1}{(4\pi)^2} \frac{e^3}{2 \sin^3 \theta_W} C_{tb} C_{ts}^* \frac{1}{M_W^2}. \quad (46)$$

The property $C_{cs}^* C_{cb} \approx -C_{ts}^* C_{tb}$ for the 3×3 CKM matrix has been used in the previous equation. The inclusive width for $b \rightarrow s + \gamma$ decay is finally given by

$$\Gamma(b \rightarrow s + \gamma) = \frac{m_b^5}{16\pi} |F_2(m_b)|^2 \quad (47)$$

Where we have neglected the phase-space factor of order $O(\frac{m_s^2}{m_b^2})$. We calculate the corresponding branching ratio as in Ref [19] by making use of the semileptonic decay $b \rightarrow ce\bar{\nu}$, one gets:

$$Br(b \rightarrow s + \gamma) = \frac{\Gamma(b \rightarrow s + \gamma)}{\Gamma(b \rightarrow ce\bar{\nu})} Br(b \rightarrow ce\bar{\nu}) \quad (48)$$

where for $Br(b \rightarrow ce\bar{\nu})$ we use the averaged experimental value 0.11 [20]. The QCD-corrected width for the semileptonic decay $b \rightarrow ce\bar{\nu}$ is [21]

$$\Gamma(b \rightarrow ce\bar{\nu}) = \frac{G_F^2 m_b^5}{192\pi^3} \rho(\frac{m_c}{m_b}, 0, 0) |C_{bc}|^2 \{1 - \frac{2\alpha_s(m_b)}{3\pi} f(\frac{m_c}{m_b}, 0, 0)\} \quad (49)$$

where the phase-space factor ρ is 0.447 and $f(\frac{m_c}{m_b}, 0, 0) = 2.41$, G_F is the Fermi constant.

C. The width of $b \rightarrow se^+e^-$ in SUSY model with bilinear R-parity violation

This decay has been often considered the benchmark of charmless b-decays with strange particles in the final state. We will provide below the amplitude for $b \rightarrow se^+e^-$ including QCD effects. In what follows, the same conventions as in the previous decay have been adopted.

We begin by considering the diagrams which induce the effective flavor-changing coupling of the photon to quarks (photon penguins). They are given by the diagrams shown in Fig. 1 with a lepton line attached to the photon propagator. We consider separately the monopole (LL) and dipole (LR) form factor, which are related to different effective operators.

(i) Photon penguins (LL component, at the M_W scale)

$$\begin{aligned}
\mathcal{A}_{tot}^{\gamma,LL}(b \rightarrow se^+e^-) &= eF_1\mathcal{O}_{LLV} \\
&\equiv F_1^\gamma\mathcal{O}_{LLV}
\end{aligned} \tag{50}$$

where $\mathcal{O}_{LLV} = (\bar{s}\gamma^\mu P_L b)(\bar{e}\gamma_\mu e)$ and F_1 is the sum of Eq. (27), Eq. (29), Eq. (31), Eq. (33), Eq. (35).

(ii) Photon penguins (LR component, at the M_W scale)

$$\begin{aligned}
\mathcal{A}_{tot}^{\gamma,LR}(b \rightarrow se^+e^-) &= eF_2\mathcal{O}_{LRV} \\
&\equiv F_2^\gamma\mathcal{O}_{LRV}
\end{aligned} \tag{51}$$

with F_2 is the sum of Eq. (28), Eq. (30), Eq. (32), Eq. (34), Eq. (36) and the operator \mathcal{O}_{LRV} is defined as:

$$\mathcal{O}_{LRV} \equiv m_b \frac{1}{q^2} (\bar{s} \not{q} \gamma^\mu P_R b) (\bar{e} \gamma_\mu e)$$

(iii) Z^0 - penguins. The process $b \rightarrow se^+e^-$ is also induced by the effective FC coupling of the Z^0 to quarks. The total amplitude coming from the Z^0 -penguins can be expressed as (at the M_W scale)

$$\begin{aligned}
\mathcal{A}_{tot}^Z(b \rightarrow se^+e^-) &= \frac{e}{M_Z^2 \sin \theta_W \cos \theta_W} \Gamma_Z \left(-\frac{1}{2} \mathcal{O}_{LLL} + \sin^2 \theta_W \mathcal{O}_{LLV} \right) \\
&\equiv A^Z \left(-\frac{1}{2} \mathcal{O}_{LLL} + \sin^2 \theta_W \mathcal{O}_{LLV} \right)
\end{aligned} \tag{52}$$

where the new operator \mathcal{O}_{LLL} is given as

$$\mathcal{O}_{LLL} = (\bar{s}\gamma^\mu P_L b)(\bar{e}\gamma_\mu P_L e)$$

and $\Gamma_Z = \sum \Gamma_Z^{(i)}$ is the sum of Eq. (21), Eq. (22), Eq. (23), Eq. (24) and Eq. (25).

(iv) Box diagrams. The relevant contributions are given in Eq. (39), Eq. (40).

In order to implement the QCD corrections, let us rewrite the total amplitude at the M_W scale as:

$$\mathcal{A}_{tot}^{(b \rightarrow se^+e^-)}(M_W) = A_{LLV}(M_W)\mathcal{O}_{LLV} + A_{LRV}(M_W)\mathcal{O}_{LRV} + A_{LLL}(M_W)\mathcal{O}_{LLL} \tag{53}$$

with

$$\begin{aligned}
A_{LLV}(M_W) &= F_1^\gamma + \sin^2 \theta_W A^Z, \\
A_{LRV}(M_W) &= F_2^\gamma, \\
A_{LLL}(M_W) &= -A^Z/2 + (A_a^{box} + A_b^{box}).
\end{aligned} \tag{54}$$

Renormalization at the m_b -scale leads to [22]

$$\begin{aligned}
A_{LLV}(m_b) &= A_{LLV}^\gamma(M_W) + \sin^2 \theta_W A^Z(M_W) + A'_0 \frac{4\pi}{\alpha_s(M_W)} \left\{ \frac{8}{87} [1 - \eta^{-\frac{29}{23}}] \right. \\
&\quad \left. - \frac{4}{33} [1 - \eta^{-\frac{11}{23}}] \right\} - \frac{4}{9} A'_0 \left[\ln\left(\frac{m_c^2}{m_b^2}\right) + f(s) \right] \left[2\eta^{-\frac{6}{23}} - \eta^{\frac{12}{23}} \right],
\end{aligned} \tag{55}$$

$$A_{LRV}(m_b) = \eta^{-\frac{16}{23}} \{ A_{LRV}(M_W) + A'_0 \left[\frac{116}{135} (\eta^{\frac{10}{23}} - 1) + \frac{58}{189} (\eta^{\frac{28}{23}} - 1) \right] \}, \tag{56}$$

$$A_{LLL}(m_b) = A_{LLL}(M_W), \tag{57}$$

where $A'_0 = F_2^0 \sqrt{4\pi\alpha}$ and η, F_2^0 have been defined in Eq. (46) .

The differential decay rate is then given by [15]:

$$\begin{aligned}
\frac{d\Gamma}{ds} &= \frac{m_b^5}{1536\pi^3} 4(1-s^2) \left\{ \left(\frac{1}{2} + s \right) [|A_{LLV} + A_{LLL}|^2 + |A_{LLV}|^2] \right. \\
&\quad \left. + \left(1 + \frac{2}{s} \right) |A_{LRV}|^2 - 3Re[(2A_{LLV} + A_{LLL})A_{LRV}^*] \right\}
\end{aligned} \tag{58}$$

where $s = \frac{q^2}{m_b^2}$.

D. The width of $b \rightarrow s \sum \nu_i \bar{\nu}_i$ in SUSY model with bilinear R-parity violation

The transition $b \rightarrow s \sum \nu_i \bar{\nu}_i$ is induced by Z^0 -penguins and box diagrams, which, at the leading order, lead to the same effective operator. The peculiarity of this process is that it is not affected by the QCD renormalization. This is simply understood by noticing that the current $(\bar{s}\gamma^\mu P_L b)$ is conserved in the limit of vanishing quark masses. Conserved currents have canonical dimensions and no divergent counterterms arise. This ultraviolet behavior is not spoiled by consideration of finite quark masses [15].

The original electroweak sensitivity to the top mass is therefore preserved. On the other hand, the experimental search for this rare B- transition is understandably much harder than for the previous semileptonic decay.

For the e-neutrino and μ -neutrino, we obtain the following result

$$\mathcal{A}_{tot}(b \rightarrow s\nu_i\bar{\nu}_i(i = e, \mu)) = A^\nu \mathcal{O}_{LLL}^\nu, \quad (59)$$

where $A^\nu = A^Z + B_a^{box} + B_b^{box}$ with $A^Z = \frac{e}{\sin\theta_W \cos\theta_W} \Gamma_Z$ and $B_{a,b}^{box}$ is given in Eq. (42) and Eq. (43). The decay rate for the e, μ -neutrino is then given by

$$\Gamma(b \rightarrow s\nu_i\bar{\nu}_i(i = e, \mu)) = \frac{m_b^5}{1536\pi^3} |A_{LLL}^\nu|^2. \quad (60)$$

As for the τ -neutrino, the case is complicated because the τ -neutrino mixed with the neutralinos under our assumption. The interaction between the Z_0 boson and τ -neutrino can be written as:

$$\mathcal{L}_{int}^{Z_0-\bar{\nu}_\tau-\nu_\tau} = -\frac{e}{2\sin\theta_W \cos\theta_W} Z_\mu \bar{\nu}_\tau \gamma^\mu P_L \nu_\tau \{|Z_N^{3,1}|^2 - |Z_N^{4,1}|^2 + |Z_N^{5,1}|^2\}, \quad (61)$$

where Z_N is the mixing matrix of τ -neutrino and neutralinos, its definition can be found in the appendix. C. For the τ -neutrino, we have

$$\mathcal{A}_{tot}(b \rightarrow s\nu_\tau\bar{\nu}_\tau) = F_{mix} A^\nu \mathcal{O}_{LLL}^\nu \quad (62)$$

with

$$F_{mix} = |Z_N^{3,1}|^2 - |Z_N^{4,1}|^2 + |Z_N^{5,1}|^2. \quad (63)$$

The decay rate for the τ -neutrino is given as:

$$\Gamma(b \rightarrow s\nu_\tau\bar{\nu}_\tau) = \frac{m_b^5}{1536\pi^3} F_{mix}^2 |A_{LLL}^\nu|^2, \quad (64)$$

here we neglect the mass of τ -neutrino. We may now sum over all three types neutrino species:

$$\Gamma(b \rightarrow s \sum \nu_i \bar{\nu}_i) = \frac{m_b^5}{1536\pi^3} (2 + F_{mix}^2) |A_{LLL}^\nu|^2. \quad (65)$$

As we shall see in the next section this leads to a rate for $b \rightarrow s \sum \nu_i \bar{\nu}_i$ which is about four times larger than the rate for $b \rightarrow se^+e^-$.

IV. NUMERICAL RESULTS

In this section, we will compute the branch ratio of the processes that have been analyzed in sect. III. In the numerical evaluation below, we take $\alpha = \frac{e^2}{4\pi} \approx \frac{1}{128.8}$, $\alpha_s(M_W) \approx 0.118$, $m_e \approx 0.511\text{MeV}$, $m_\tau \approx 1.777\text{GeV}$, $M_Z \approx 91.187\text{GeV}$, $M_W \approx 80.330\text{GeV}$, $m_t \approx 174\text{GeV}$, $m_c \approx 1.3\text{GeV}$ and $m_b \approx 4.3\text{GeV}$.

In order to find out the allowed region in the parameter space, one has to take a number of constraint into account. First, we note that m_1 , m_2 , ϵ_3 , μ , $\tan\beta$, $\tan\theta_v$ and l_3 are the parameters that enter into the chargino and neutralino mass matrices. The strongest constraint on them follows from the fact that the τ mass has been experimentally measured [20], therefore, for any combination of those parameters, the lowest eigenvalue of Eq. (18) should agree with m_τ . Also, ν_τ has a laboratory upper limit of 24MeV on its mass. The two restrictions, together with the positive-definite condition of the mass squared matrices, constrain the parameter space in a severe manner.

We open our discussion by considering the experimental results of rare B processes impact on the mass spectrum in the model. At present, the experimental bound on the $b \rightarrow s\gamma$, $b \rightarrow sl^+l^-$ are $2 \times 10^{-4} \leq Br(b \rightarrow s + \gamma) \leq 4.5 \times 10^{-4}$ [20] and $Br(b \rightarrow se^+e^-)^{CLEO} \leq 5.7 \times 10^{-5}$ [23] respectively. Not having the generality lost, we assume $l_{s3} = l_3$ in the numerical calculation and the value of l_3 can be determined from $Det|m_\tau^2 - \mathcal{M}_f^\dagger \mathcal{M}_f| = 0$ when the relevant parameters are given. Furthermore, we interest the constraint on the mass spectrum that is imposed by the experimental results of rare B processes, so we take the range of the parameters as:

$$\begin{aligned}
-500\text{GeV} &\leq B, B_3 \leq 500\text{GeV}, \\
10^4\text{GeV}^2 &\leq m_{RI}^2, m_{QI}^2, m_{UI}^2, m_{DI}^2 \leq 4 \times 10^6\text{GeV}^2, \\
100\text{GeV} &\leq m_1, m_2 \leq 1000\text{GeV}, \\
-1000\text{GeV} &\leq \mu \leq 1000\text{GeV}.
\end{aligned} \tag{66}$$

In the numerical program, the other parameters such as $\tan\beta$, $\tan\theta_v$ etc. are given in the

figure caption. In Fig. 4, we plot the lightest charged Higgs mass versus ϵ_3 (in GeV). Under the bound of rare B processes, we find the value of M_{H^+} can vary from 100GeV to about 800GeV when the parameters vary. Fig. 5 shows the lightest chargino mass varies with the parameter ϵ_3 , with other parameters taken as above. The point we should note is that $m_{\tilde{\kappa}_2^+}$ should be heavy when the $\tan\theta_v$ taken large value (such as $\tan\theta_v \sim 20$). When the $\tan\theta_v$ taken small value, the mass of $\tilde{\kappa}_2^+$ can vary from 30GeV to several hundreds GeV.

Now, we turn to discuss the branch ratios of rare B processes. From Eq. (14), we find the parameters B , B_3 enter the mass matrix of charged Higgs (just as in the mass matrices of CP-odd Higgs and CP-even Higgs) in forms $B\mu$ and $B_3\epsilon_3$. Because we are interest in relatively light charginos and scalar particles, we take

$$\begin{aligned}
-100\text{GeV} &\leq B \leq 100\text{GeV}, \\
-100\text{GeV} &\leq B_3 \leq 100\text{GeV}, \\
10^4\text{GeV}^2 &\leq m_{R^I}^2, m_{Q^I}^2, m_{U^I}^2, m_{D^I}^2 \leq 2.5 \times 10^5\text{GeV}^2, \\
100\text{GeV} &\leq m_1, m_2 \leq 500\text{GeV}, \\
-500\text{GeV} &\leq \mu \leq 500\text{GeV}.
\end{aligned} \tag{67}$$

In Fig. 6 we plot the branching ratio of $b \rightarrow s + \gamma$ as a function ϵ_3 under some different value of $\tan\beta$ and $\tan\theta_v$. The dependence on the remnant SUSY parameter such as μ , m_1 , m_2 is represented by the vertical width of the band. We see that positive interference with the different sources of SUSY contributions can produce an intensive enhancement over the QCD- corrected SM prediction (horizontal solid line) when those parameters are assigned suitable values. Sometimes, the supersymmetric contributions dominate over the SM contributions resulting in significant deviation from the SM prediction.

Let us discuss the semileptonic FCNC decay $b \rightarrow s + e^+e^-$ and $b \rightarrow s \sum \nu_i \bar{\nu}_i$ numerically. In the SM, the QCD-corrected $Br(b \rightarrow s + e^+e^-)$ is about 9×10^{-6} . The addition of the one-loop contributions where SUSY particles are present modify the prediction up to about four times the SM prediction as it can be gathered from Fig. 7. The CLEO collaboration has already been searched for inclusive $b \rightarrow sl^+l^-$ ($l = e, \mu$). The results are [23]:

$$\begin{aligned}
Br(b \rightarrow se^+e^-)^{CLEO} &\leq 5.7 \times 10^{-5}, \\
Br(b \rightarrow s\mu^+\mu^-)^{CLEO} &\leq 5.8 \times 10^{-5}.
\end{aligned}
\tag{68}$$

By comparing the numerical result with experiment, we find that we can not excluded the large value of ϵ_3 . Analogous considerations hold for $b \rightarrow s \sum \nu_i \bar{\nu}_i$ (Fig. 8). The R-breaking terms can have an appreciable effect for the $b \rightarrow s \sum \nu_i \bar{\nu}_i$. This is the main difference between the BRPV model and the usual SUSY model with R-parity.

In summary, as a simple extension of the MSSM which introduce R-parity violation, the R-breaking terms in BRPV model can give an appreciable effect for the rare B-processes. From the present experimental bound on those processes, we can get some constraint on the mass spectrum in this model under some suitable assumptions.

Acknowledgment This work was supported in part by the National Natural Science Foundation of China and the Grant No. LWLZ-1298 of the Chinese Academy of Sciences.

APPENDIX A: THE DEFINITION OF VARIOUS FUNCTIONS

We collect in this appendix the various functions that were used in the text. The one-variable functions obtained from the penguin diagrams are given as:

$$\begin{aligned}
f_2^{(0)}(x) &= \frac{x}{1-x} \ln x, \\
f_{3a}^{(0)}(x) &= -\frac{1}{1-x} \left\{ 1 + \frac{x}{1-x} \ln x \right\}, \\
f_{3b}^{(0)}(x) &= \frac{1}{1-x} \left\{ 1 + \frac{1}{1-x} \ln x \right\}, \\
f_{3a}^{(1)}(x) &= \frac{2 \ln x}{1-x} + \ln x - \frac{\ln x}{(1-x)^2} - \frac{1}{(1-x)}, \\
f_{3b}^{(1)}(x) &= \frac{2x \ln x}{1-x} - \ln x + \frac{x^2 \ln x}{(1-x)^2} + \frac{x}{(1-x)},
\end{aligned}$$

$$\begin{aligned}
f_{4a}^{(1)}(x) &= \frac{1}{(x-1)} \left[\frac{1}{2} + \frac{x}{x-1} - \frac{x^2}{(x-1)^2} \ln x \right], \\
f_{4b}^{(1)}(x) &= \frac{2}{(x-1)} \left[\frac{1}{2} - \frac{x}{x-1} - \frac{x}{(x-1)^2} \ln x \right], \\
f_{4c}^{(1)}(x) &= -\frac{1}{(x-1)} \left[\frac{1}{2} - \frac{1}{x-1} - \frac{1}{(x-1)^2} \ln x \right], \\
f_{5a}^{(2)}(x) &= \frac{1}{3(x-1)} + \frac{x}{2(x-1)^2} + \frac{x^2}{(x-1)^3} - \frac{x^3}{(x-1)^4} \ln x, \\
f_{5b}^{(2)}(x) &= \frac{5}{2(x-1)} - \frac{3x}{2(x-1)^2} + \frac{3x^2}{(x-1)^3} - \frac{3x^2}{(x-1)^4} \ln x, \\
f_{5c}^{(2)}(x) &= -\frac{1}{2(x-1)} + \frac{3x}{2(x-1)^2} + \frac{3}{(x-1)^3} - \frac{3x}{(x-1)^4} \ln x, \\
f_{5d}^{(2)}(x) &= -\frac{1}{3(x-1)} + \frac{1}{2(x-1)^2} - \frac{1}{(x-1)^3} + \frac{1}{(x-1)^4} \ln x.
\end{aligned} \tag{A1}$$

The two- and three-variable functions obtained from penguin and box diagrams are

$$\begin{aligned}
f_{3c}^{(0)}(x, y) &= -\frac{1}{x-y} \left[\frac{x}{x-1} \ln x - \frac{y}{y-1} \ln y \right], \\
f_{3c}^{(1)}(x, y) &= -\frac{1}{2(x-y)} \left[\frac{x^2}{x-1} \ln x - \frac{y^2}{y-1} \ln y \right], \\
f_{4d}^{(1)}(x, y) &= \frac{1}{x-y} \left[\frac{x^2}{(x-1)^2} \ln x - \frac{1}{x-1} - (x \rightarrow y) \right], \\
f_{4e}^{(1)}(x, y, z) &= \frac{1}{x-y} \left\{ \frac{1}{x-z} \left[\frac{x^2}{(x-1)} \ln x - \frac{3x}{2} - (x \rightarrow z) \right] - (x \rightarrow y) \right\}.
\end{aligned} \tag{A2}$$

APPENDIX B: THE RELEVANT FEYNMAN RULES IN SUSY MODEL WITH BILINEAR R-PARITY VIOLATION

In this appendix, we give some relevant Feynman rules in the supersymmetric model with bilinear R-parity violation that were used in the paper.

It is first convenient to introduce the mixing matrices relative to the scalar-quark sector. We denote with $\tilde{Q}_{L,R}^I$ the squark current eigenstates (where $I = 1, 2, 3$ is the generation label and $Q = U, D$), and with $\tilde{Q}_{1,2}^I$ the corresponding mass eigenstates of the I-th generation (we neglect the generation-mixing of the scalar-quark and scalar-lepton). The 2×2 mixing matrices $Z_{\tilde{Q}^I}$ are defined by

$$\begin{aligned}
\tilde{Q}_L^I &= Z_{\tilde{Q}^I}^{1,i} \tilde{Q}_i^I, \\
\tilde{Q}_R^I &= Z_{\tilde{Q}^I}^{2,i} \tilde{Q}_i^I.
\end{aligned} \tag{B1}$$

Similar, the 2×2 mixing matrices $Z_{\tilde{E}^I}$ are defined as

$$\begin{aligned}
\tilde{L}^I &= Z_{\tilde{E}^I}^{1,i} \tilde{E}_i^I, \\
\tilde{R}^{I*} &= Z_{\tilde{E}^I}^{2,i} \tilde{E}_i^I
\end{aligned} \tag{B2}$$

with \tilde{L}^I , \tilde{R}^I are the slepton current eigenstates and $\tilde{E}_{1,2}^I$ are the corresponding mass eigenstates. The S_i , ($S_{i=1,2,3,4} = G^-, H^-, \tilde{\tau}_1, \tilde{\tau}_2$) up quark and down quark couplings can be written as (Fig. 9)

$$i \left[\frac{em_d^I}{\sqrt{2}M_W \sin \theta_W \sin \theta_v \cos \beta} Z_H^{1i} P_L + \frac{em_u^J}{\sqrt{2}M_W \sin \theta_W \sin \theta_v \sin \beta} Z_H^{2i} P_R \right] C_{IJ}. \tag{B3}$$

The couplings of down quark, up scalar quark and chargino are given by (Fig. 10)

$$\begin{aligned}
& i \left[\left(\frac{-e}{\sin \theta_W} Z_{\tilde{U}^I}^{1i*} Z_{1j}^+ + \frac{em_u^J}{\sqrt{2}M_W \sin \theta_W \sin \theta_v \sin \beta} Z_{\tilde{U}^I}^{2i*} Z_{2j}^+ \right) P_L + \right. \\
& \left. \frac{em_d^I}{\sqrt{2}M_W \sin \theta_W \sin \theta_v \cos \beta} Z_{\tilde{U}^J}^{1i*} Z_{2j}^- P_R \right] C_{IJ}^*.
\end{aligned} \tag{B4}$$

The couplings of up quark, down scalar quark and chargino are given by (Fig. 11)

$$\begin{aligned}
& i \left[\left(\frac{-e}{\sin \theta_W} Z_{\tilde{D}^I}^{1i} Z_{1j}^+ + \frac{em_d^I}{\sqrt{2}M_W \sin \theta_W \sin \theta_v \cos \beta} Z_{\tilde{D}^I}^{2i} Z_{2j}^- \right) P_L + \right. \\
& \left. \frac{em_u^J}{\sqrt{2}M_W \sin \theta_W \sin \theta_v \sin \beta} Z_{\tilde{D}^I}^{1i} Z_{2j}^{+*} P_R \right] C_{IJ}^*.
\end{aligned} \tag{B5}$$

The couplings of Z^0 and S_i are (Fig. 12)

$$i \frac{e}{2 \sin \theta_W \cos \theta_W} [(\cos^2 \theta_W - \sin^2 \theta_W) \delta_{ij} - Z_H^{4i} Z_H^{4j*}] (p + k)^\mu, \tag{B6}$$

where $S_i = (G^-, H^-, \tilde{\tau}_1, \tilde{\tau}_2)$, $i = 1, 2, 3, 4$. The matrices Z_H , Z^\pm have been defined as above.

APPENDIX C: THE MIXING BETWEEN τ -NEUTRINO AND NEUTRALINOS

In this appendix, we give the mass matrix of τ -neutrino and neutralinos under our assumption.

From Eq. (5) and Eq. (7), the τ neutrino-neutralino mass terms in the Lagrangian are

$$\mathcal{L}_{neutralino} = -\frac{1}{2}(\Psi^0)^T \mathcal{M}_N \Psi^0 + h.c. \quad (C1)$$

with $(\Psi^0)^T = (-i\lambda_B, -i\lambda_A^3, \psi_{H^1}^1, \psi_{H^2}^2, \nu_{\tau_L})$ and

$$\mathcal{M}_N = \begin{pmatrix} 2m_1 & 0 & -\frac{1}{2}g'v_1 & \frac{1}{2}g'v_2 & -\frac{1}{2}g'v_3 \\ 0 & 2m_2 & \frac{1}{2}gv_1 & -\frac{1}{2}gv_2 & \frac{1}{2}gv_3 \\ -\frac{1}{2}g'v_1 & \frac{1}{2}gv_1 & 0 & -\frac{1}{2}\mu & 0 \\ \frac{1}{2}g'v_2 & -\frac{1}{2}gv_2 & -\frac{1}{2}\mu & 0 & \frac{1}{2}\epsilon_3 \\ -\frac{1}{2}g'v_3 & \frac{1}{2}gv_3 & 0 & \frac{1}{2}\epsilon_3 & 0 \end{pmatrix} \quad (C2)$$

The formulae of mixing matrix are:

$$\begin{aligned} -i\lambda_B &= Z_N^{1,i} \chi_i^0, \\ -i\lambda_A^3 &= Z_N^{2,i} \chi_i^0, \\ \psi_{H^1}^1 &= Z_N^{3,i} \chi_i^0, \\ \psi_{H^2}^2 &= Z_N^{4,i} \chi_i^0, \\ \nu_{\tau_L} &= Z_N^{5,i} \chi_i^0 \end{aligned} \quad (C3)$$

and

$$\nu_\tau = \begin{pmatrix} \chi_1^0 \\ \bar{\chi}_1^0 \end{pmatrix} \quad (C4)$$

$$\kappa_i^0 = \begin{pmatrix} \chi_{i+1}^0 \\ \bar{\chi}_{i+1}^0 \end{pmatrix} \quad (C5)$$

with $i = 1, 2, 3, 4$. Here, we identify the ν_τ as the lightest mass eigenstate of the mass matrix. The matrix Z_N satisfies the following condition: $Z_N^T \mathcal{M}_N Z_N = \text{diag}(m_{\nu_\tau}, m_{\kappa_1^0}, m_{\kappa_2^0}, m_{\kappa_3^0}, m_{\kappa_4^0})$. Similar to the mixing matrices of τ -chargino sector, we can assume $m_{\nu_\tau}, m_{\kappa_i^0}$ ($i = 1, 2, 3, 4$) positive and $m_{\kappa_4^0} > m_{\kappa_3^0} > m_{\kappa_2^0} > m_{\kappa_1^0} > m_{\nu_\tau}$.

REFERENCES

- [1] For reviews see, for example, H.P.Nilles, Phys. Rep.110, 1(1984); H. E. Haber and G. L. Kane, *ibid* 117,75(1985).
- [2] See, for example, R.Barbieri and L. Hall, Phys. Lett. B238, 86(1990); V. Barger et al. Phys. Rev. D44, 1629(1991); R. Godbole, P. Roy and X. Tata, Nucl. Phys. B401, 67(1993).
- [3] S. Roy and B. Mukhopadhyaya, Phys. Rev. D55, 7020(1997); R. Hempfling, Nucl. Phys. B478, 3(1996); B. de Carlos, P. L. White, Phys. Rev. D55, 4222(1997).
- [4] C. S. Aulakh and R. N. Mohapatra, Phys. Lett. 119B, 136(1982); A. Masiero and T. Valle, Phys. Lett, B251, 273(1990); G. Giudice et al, Nucl. Phys. B396, 243(1993); I. Umemura and K. Yamamoto, *ibid*, B423, 405(1994).
- [5] Hans. Peter Nilles and N. Polonsky, Nucl. Phys. B484, 33(1997); M. A. Diaz, J. C. Romao and J. W. F. Valle, hep-ph/9706315; Chao-Hsi Chang, Tai-Fu Feng and Lian-You Shang, hep-ph/9806505.
- [6] N. G. Deshpande, P. Lo, J. Trampetic, G. Eilam and P. Singer, Phys. Rev. Lett. 59, 183(1987); B. Grinstein, R. Springer and M. Wise, Phys. Lett. B202, 138(1988), Nucl. Phys. B339, 269(1990); R. Grigjanis, P. J. O'Donnell, M. Sutherland and H. Navelet, Phys. Lett. B213, 355(1988).
- [7] N. G. Deshpande and J. Trampetic, Phys. Rev. Lett. 60, 2583(1988); C. A. Dominguez, N. Paver and Riazuddin, Z. Phys. C48, 55(1990).
- [8] W. -S. Hou and R. S. Willey, Nucl. Phys. B236, 54(1989).
- [9] A. J. Buras, P. Krawczyk, M. E. Lautenbacher and C. Salazar, Nucl. Phys. B337, 284(1990); V.Barger, J. L. Hewett and R. J. N. Phillips, Phys. Rev. D41, 3421(1990); J. F. Gunion and B. Grzadkowski, Phys. Lett. B243, 301(1990).

- [10] D. Cocolicchio, G. Costa, G. L. Fogli, J. H. Kim and A. Masiero, Phys. Rev. D40,1477(1989).
- [11] D. London and D. Wyler, Phys. Lett. B232, 503(1989).
- [12] F. Zwirner, Phys. Lett. B132, 103(1983); J.-M. Gerard, W. Grimus, Amitava Raychaudhuri and G. Zoupanos, Phys. Lett B140, 349(1984).
- [13] M. Dugan, B. Grinstein and L. Hall, Nucl. Phys. B255, 413(1985); L. J. Hall, V. A. Kostelecky and S. Raby, Nucl. Phys. B267, 415(1986).
- [14] J. S. Hagelin, S. Kelley and T. Tanaka, Nucl. Phys. B415, 293(1994); F. Gabbiani, E. Gabrielli, A. Masiero and L. Silvestrini, Nucl. Phys. B477,321(1996).
- [15] S. Bertolini, F. Borzumati, A. Masiero and G. Ridolfi, Nucl. Phys. B353, 591(1991); F. Gabbiani and A. Masiero, Nucl. Phys. B322, 235(1989); S. Bertolini and J. Matias, hep-ph/9709330.
- [16] R. Barbieri and A. Masiero, Nucl. Phys. B267, 679(1986).
- [17] J. Erler, J. L. Feng and N. Polonsky, Phys. Rev. Lett. 78, 3063(1997); A. Masiero and L. Silvestrini, hep-ph/9711401; A. Masiero and L. Silvestrini, hep-ph/9709244.
- [18] T. Inami and C. S. Lim, Prog. of. Theo. Phys. V65, 297(1981); M. K. Gaillard, B. W. Lee and R. E. Shrock, Phys. Rev. D13, 2674(1976); E. B. Bogomol'ny, V. A. Vainstein and M. A. Shifman, Yadern Fiz. 23, 825(1976)[Soviet J. Nucl. Phys. 23, 935(1976)]; V. V. Flambaum, Yadern. Fiz. 22, 661(1975)[Soviet J. Nucl. Phys. 22, 340(1976)]; M. B. Voloshin, Yadern. Fiz. 24, 810(1976)[Soviet J. Nucl. Phys. 24, 422(1976)].
- [19] S. Bertolini, F. Borzumati and A. Masiero, Phys. Rev. Lett, 59, 180(1987).
- [20] Particle Data Group. C. Caso et al, Eur. Phys. J. C3, 1(1998).
- [21] N. Cabibbo and L. Maiani, Phys. Lett. B79, 109(1978); J. L. Cortes, X. Y. Pham and A. Tounsi, Phys. Rev. D25, 188(1982); G. L. Fogli, Phys. Rev. D28, 1153(1983).

- [22] B. Grinstein, M. J. Savage and M. B. Wise, Nucl. Phys. B319, 271(1989).
- [23] S. Glenn et al.(CELO collaboration), Phys. Rev. Lett. 80, 2289(1998).
- [24] J. Rosiek, Phys. Rev. D41, 3464(1990)
- [25] A. Ali and C. Greub, Z. Phys. C49(1991)431; A. J. Buras et al., Nucl. Phys. B424 (1994)374; M. Ciuchini et al., Phys. Lett. B316(1993)127; Nucl. Phys. B415(1994)403; G. Cella et al., Phys. Lett. B325(1994)227; M. Ciuchini et al., Phys. Lett. B334(1994)137; M. Misiak, Nucl. Phys. B393(1993)23[E. B439(1995)461]; B. Grinstein, R. Springer and M. Wise, Phys. Lett. B202(1988)138.
- [26] G. Buchalla, A. J. Buras and M. E. Lautenbacher, Rev. Mod. Phys. 68(1996); A. J. Buras, hep-ph/9806471.
- [27] S. Bertolini, F. Borzumati and A. Masiero, Phys. Rev. Lett. 59(1987)180; M. Ciuchini, E. Franco, L. Reina and L. Silvestrini, Nucl. Phys. B424(1994)374.

FIGURES

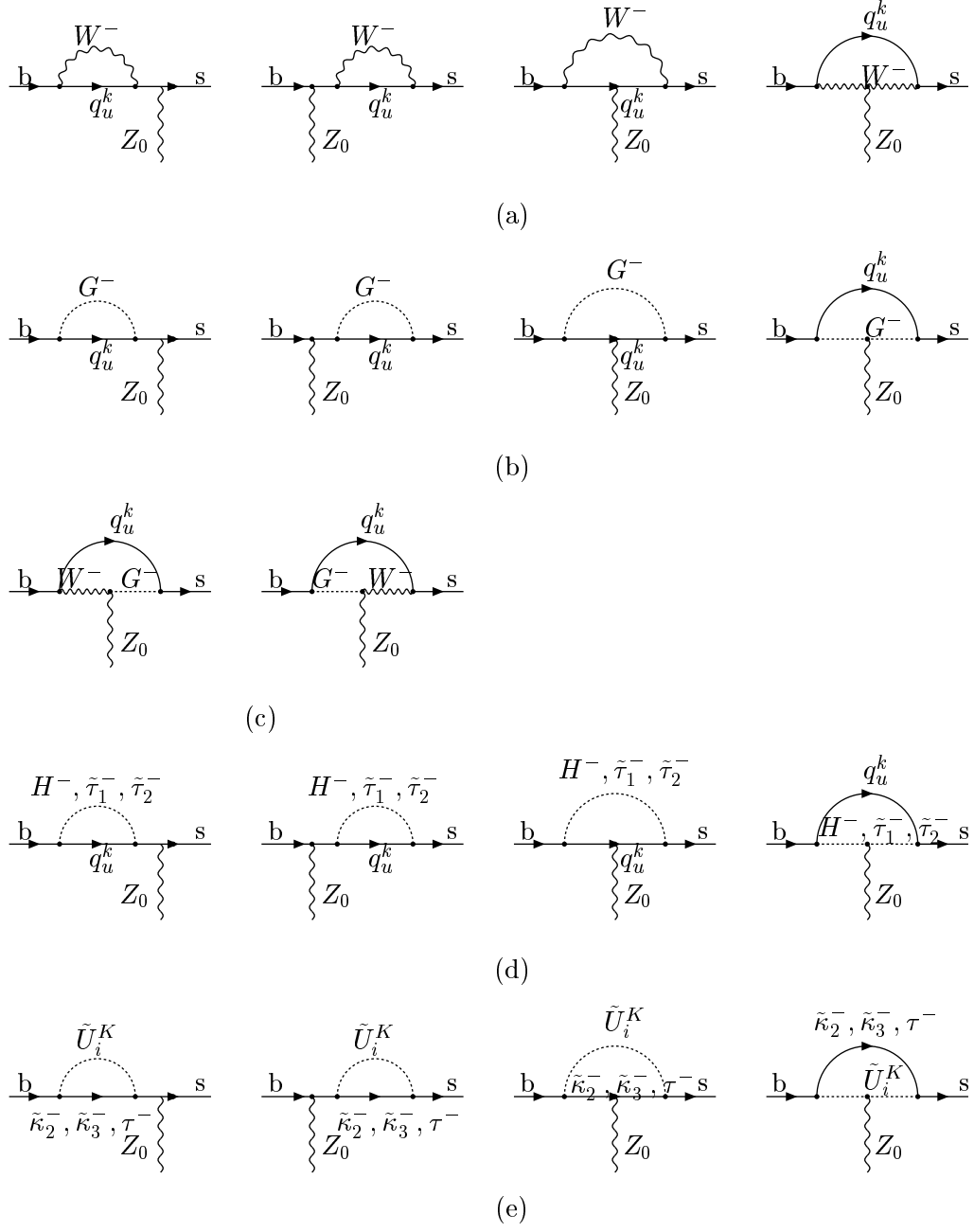


FIG. 1. The Feynman diagrams that contribute to $b\bar{s}\gamma$ and $b\bar{s}Z^0$ coupling

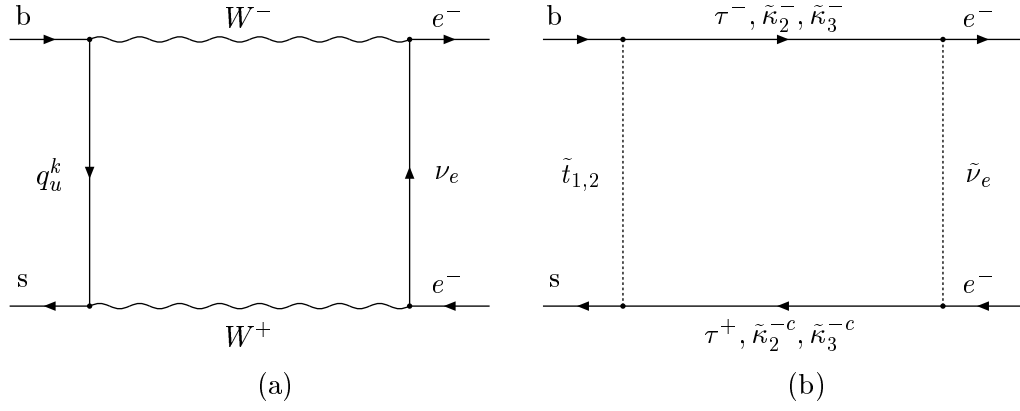


FIG. 2. The box diagrams contribute to $b \rightarrow se^+e^-$

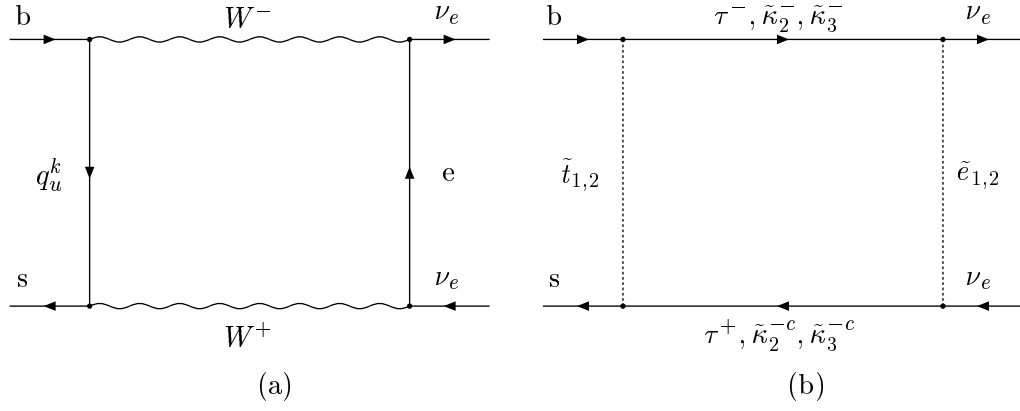
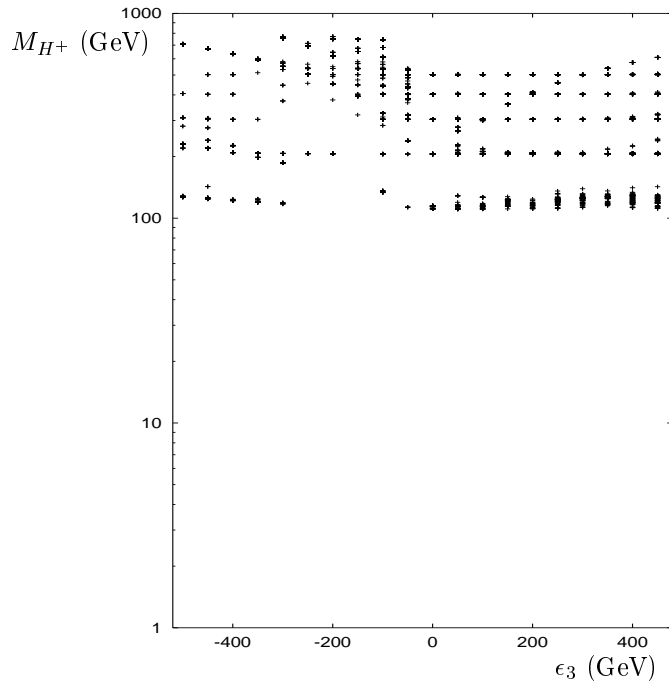
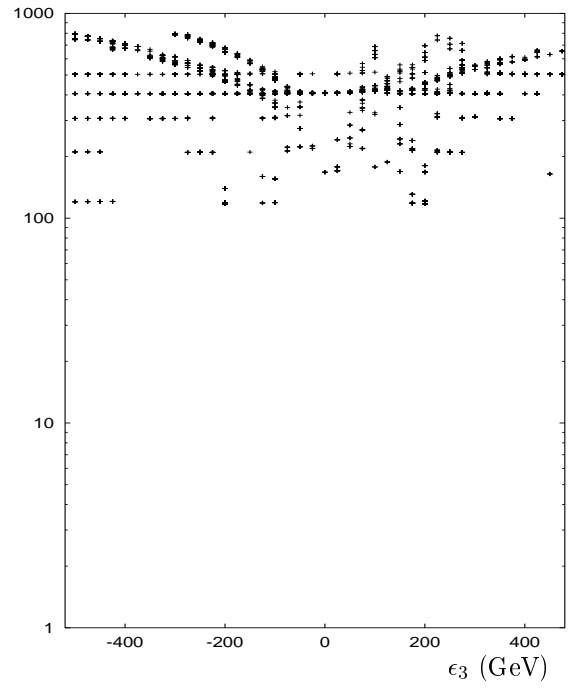


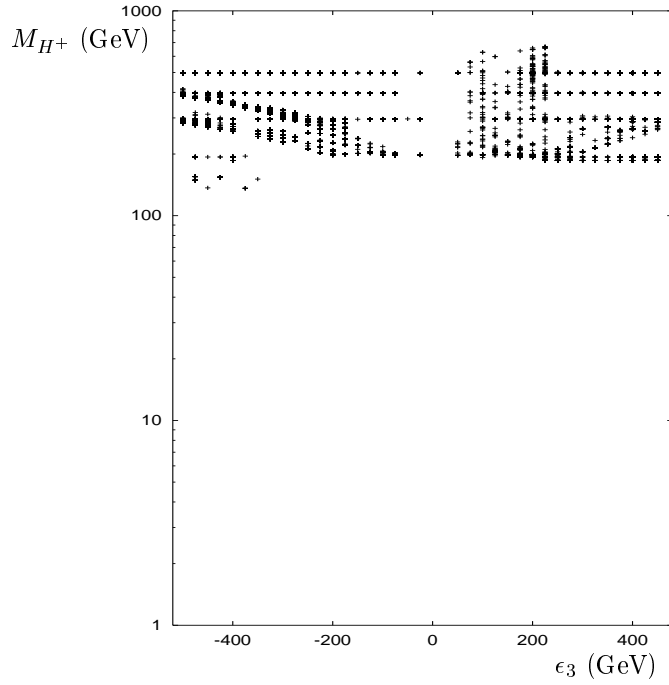
FIG. 3. The box diagrams contribute to $b \rightarrow s \nu_e \bar{\nu}_e$



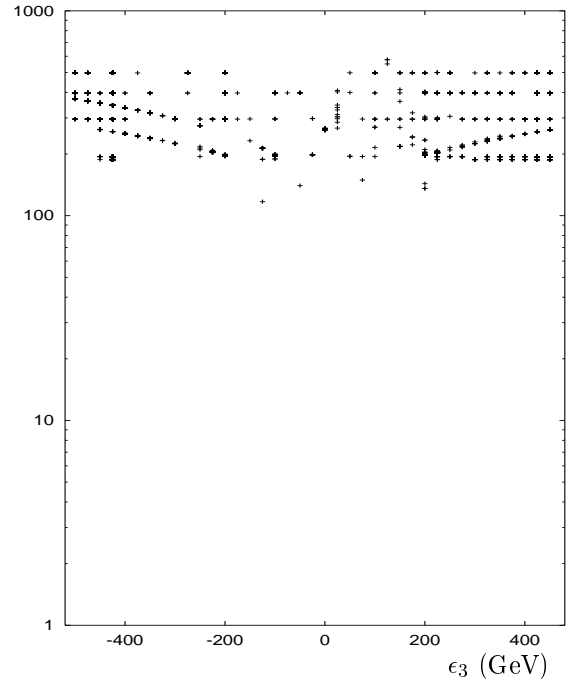
(a)



(b)

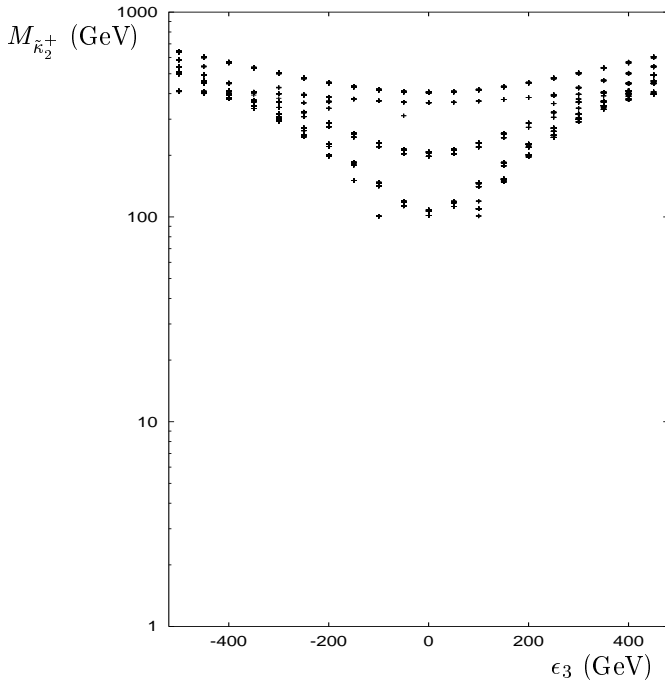


(c)

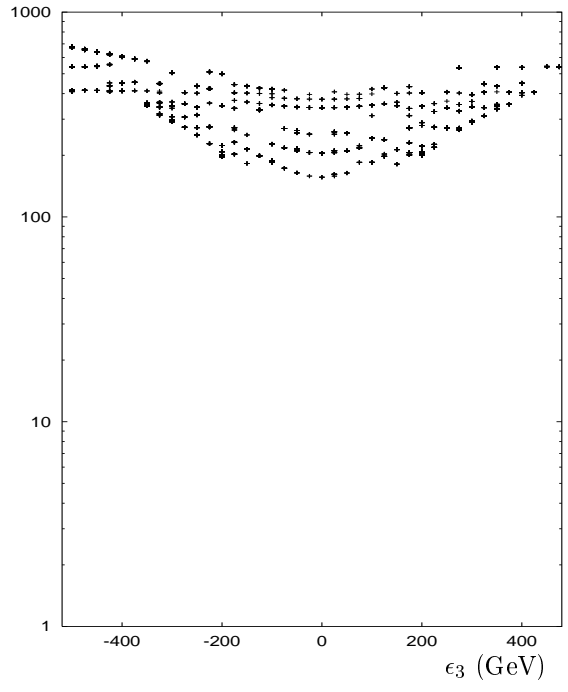


(d)

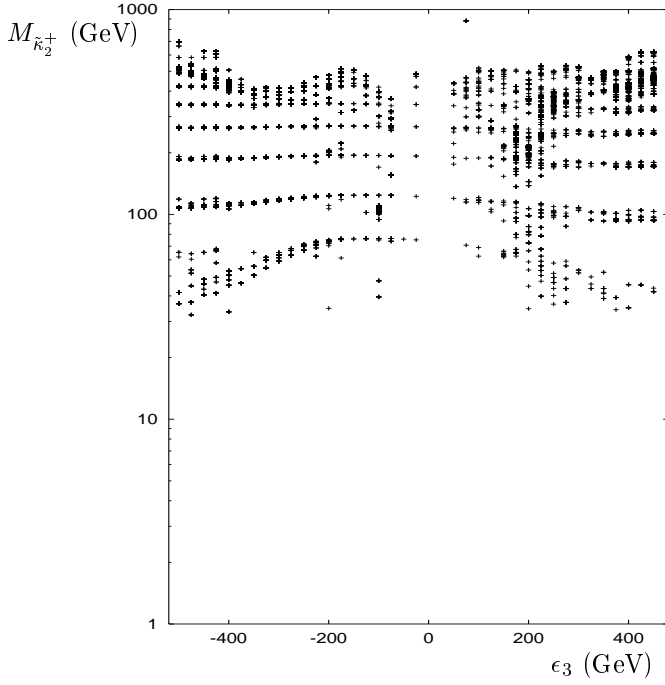
FIG. 4. Considering the experimental results of $b \rightarrow s + \gamma$, $b \rightarrow se^+e^-$, M_{H^+} vary with ϵ_3 when (a) $\tan \theta_v = 20$, $\tan \beta = 2$; (b) $\tan \theta_v = 20$, $\tan \beta = 40$; (c) $\tan \theta_v = 0.5$, $\tan \beta = 2$; (d) $\tan \theta_v = 0.5$, $\tan \beta = 40$. The other parameters are given in Eq. (66).



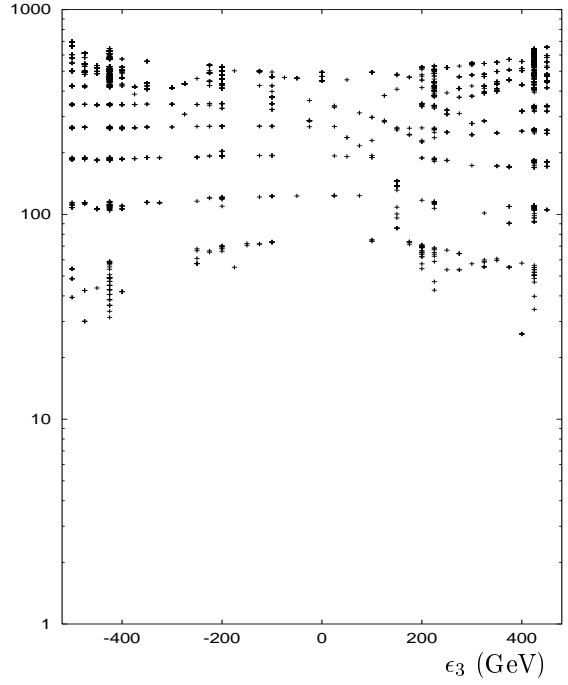
(a)



(b)



(c)



(d)

FIG. 5. Considering the experimental results of $b \rightarrow s + \gamma$, $b \rightarrow se^+e^-$, $m_{\tilde{\kappa}_2^+}$ vary with ϵ_3 when (a) $\tan \theta_v = 20$, $\tan \beta = 2$; (b) $\tan \theta_v = 20$, $\tan \beta = 40$; (c) $\tan \theta_v = 0.5$, $\tan \beta = 2$; (d) $\tan \theta_v = 0.5$, $\tan \beta = 40$. The other parameters are given in Eq. (66).

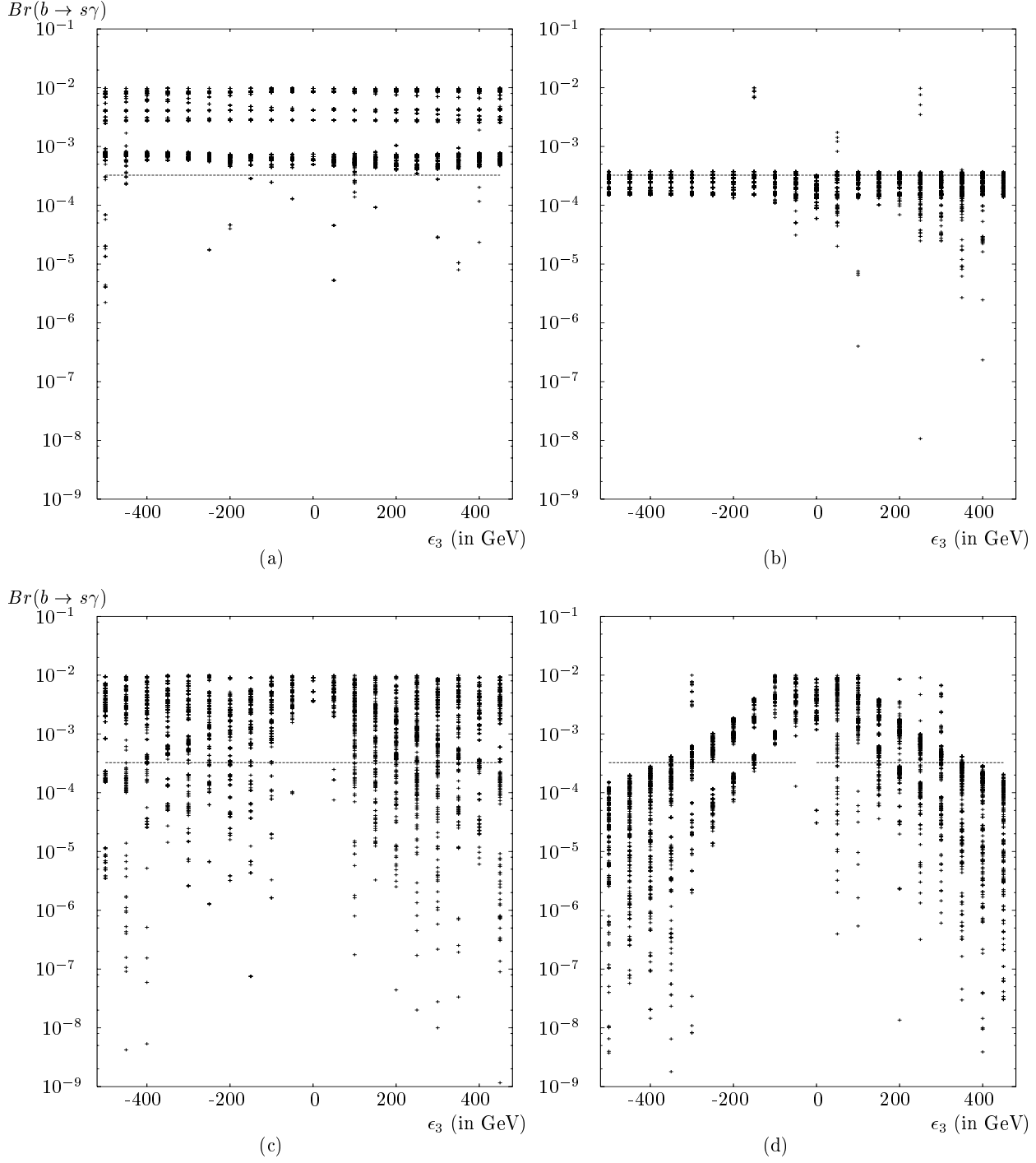


FIG. 6. Impose the Eq. (67), the branching ration of $b \rightarrow s + \gamma$ vary with ϵ_3 at the m_b -scale when (a) $\tan \theta_v = 20$, $\tan \beta = 2$; (b) $\tan \theta_v = 20$, $\tan \beta = 40$; (c) $\tan \theta_v = 0.5$, $\tan \beta = 2$; (d) $\tan \theta_v = 0.5$, $\tan \beta = 40$. The solid-lines are the predictions of SM.

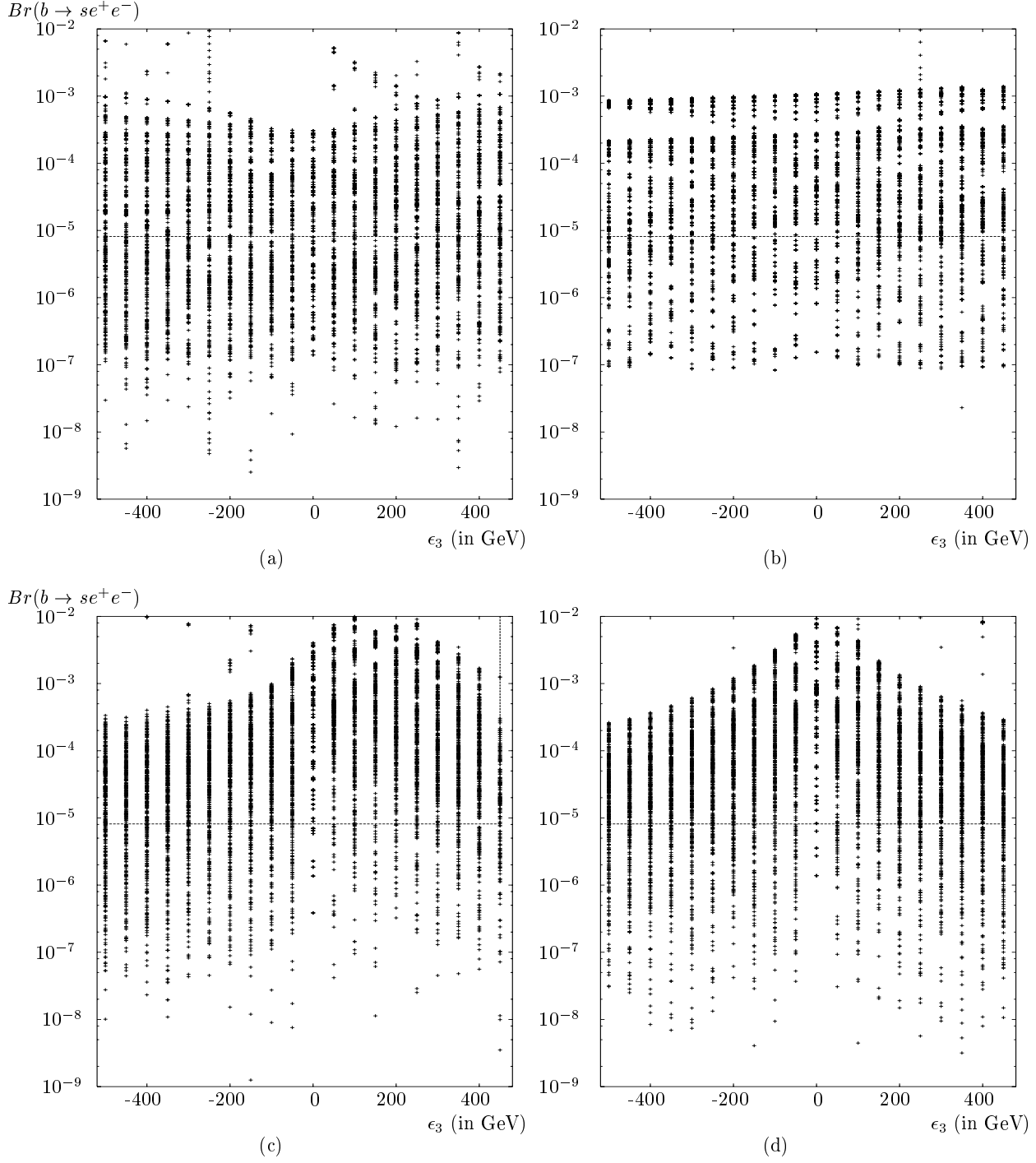


FIG. 7. Impose the Eq. (67), the branching ratio of $b \rightarrow s + e^+ e^-$ vary with ϵ_3 at the m_b -scale when (a) $\tan \theta_v = 20, \tan \beta = 2$; (b) $\tan \theta_v = 20, \tan \beta = 40$; (c) $\tan \theta_v = 0.5, \tan \beta = 2$; (d) $\tan \theta_v = 0.5, \tan \beta = 40$. The solid-lines are the predictions of SM.

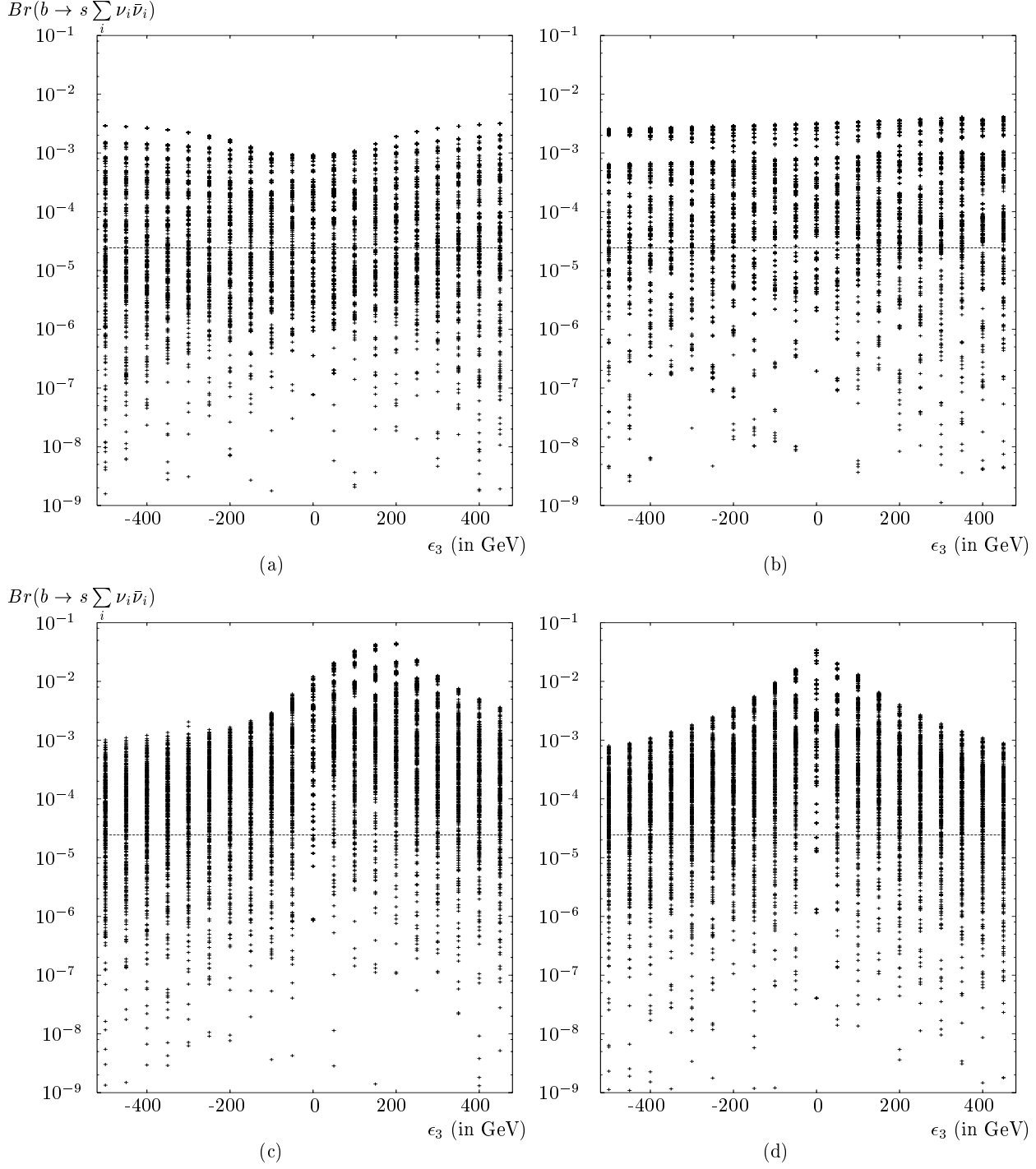


FIG. 8. Impose the Eq. (67), the branching ratio of $b \rightarrow s + \sum_i \nu_i \bar{\nu}_i$ vary with ϵ_3 at the m_b -scale when (a) $\tan \theta_v = 20, \tan \beta = 2$; (b) $\tan \theta_v = 20, \tan \beta = 40$; (c) $\tan \theta_v = 0.5, \tan \beta = 2$; (d) $\tan \theta_v = 0.5, \tan \beta = 40$. The solid-lines are the predictions of SM.

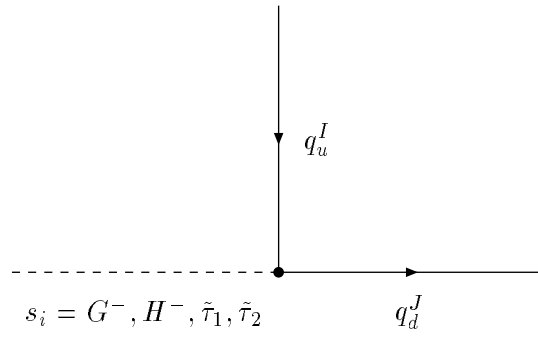


FIG. 9. The coupling between $s_i = (G^-, H^-, \tilde{\tau}_1^-, \tilde{\tau}_1^-)$ and q_u^I, q_d^J

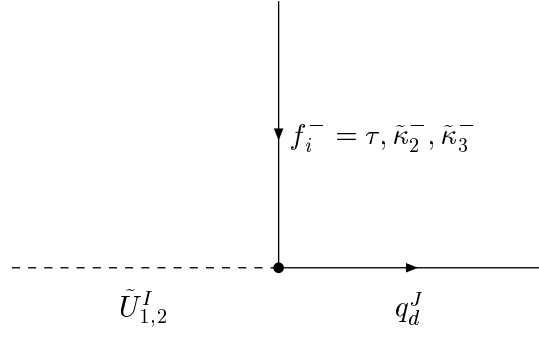


FIG. 10. The coupling between $f_i = (\tau^-, \tilde{\kappa}_2^-, \tilde{\kappa}_3^-)$ and q_d^J, \tilde{U}_j^I

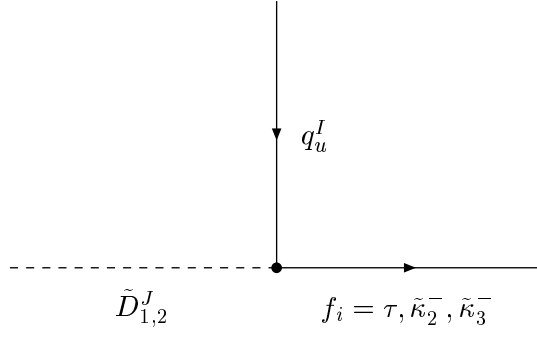


FIG. 11. The coupling between $f_i = (\tau^-, \tilde{\kappa}_2^-, \tilde{\kappa}_3^-)$ and q_u^I, \tilde{D}_j^J

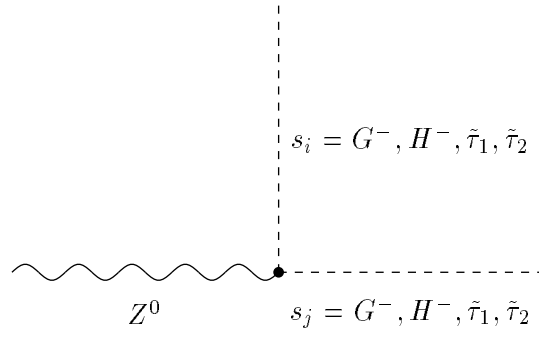


FIG. 12. The coupling between Z^0 and $s_i = (G^-, H^-, \tilde{\tau}_1, \tilde{\tau}_1)$